Supporting Information

For

Photoswitchable Architecture Transformation of a DNA-Hybrid Assembly at the Microscopic and Macroscopic Scale

Nadja A. Simeth,[a, b],‡ Paula de Mendoza,[a],‡ Victor R. A. Dubach,[c] Marc C. A. Stuart,[a, c] Julien W. Smith,[a] Tibor Kudernac,[a] Wesley R. Browne,[a] and Ben L. Feringa[a]*

[a]Stratingh Institute for Chemistry, Faculty for Science and Engineering, University of Groningen, Nijenborgh 4, 9747AG Groningen, The Netherlands.
[b]current address: Institute for Organic and Biomolecular Chemistry, University of Goettingen, Tammanstr. 2, 37077 Goettingen, Germany.
[c]Groningen Biomolecular Sciences and Biotechnology, Faculty for Science and Engineering, University of Groningen, Nijenborgh 7, 9747 AG Groningen, The Netherlands.
‡These authors contributed equally.
*b.l.feringa@rug.nl

Table of Contents

1. Synthesis and Characterization

1.1. General Remarks

Synthesis and isolation of compounds. All chemicals for synthesis were obtained from commercial sources (Sigma-Aldrich, TCI, Alfa Aesar, and Boom) and used as received unless stated otherwise. Solvents used were reagent grade for synthesis and technical grade for isolation if not otherwise stated. Dry solvents were collected from a Pure Solve MD5 solvent dispenser from Demaco or by drying them for 48 h over fresh 3 Å molecular sieves. TE buffer (1.0 mM Tris-HCl, pH 8.0, containing 0.1 mM EDTA) was purchased from Sigma-Aldrich. DNA (**dT_{20}**) was purchased and HPLC purified from BioTez. Stock solution was prepared in water. The concentration was calculated from UV-Vis absorption using extinction coefficient ε = 162600 M^{-1} cm^{-1} at 260 nm. For thin-layer chromatography (TLC) aluminum foils with a silica gel matrix (Supelco, silica gel 60, 56524) were used, and components were visualized with a UV lamp at 254 nm or through staining with NH_4CeSO_4 x H_2O (10 g/L) or ninhydrin if necessary. Flash chromatography was performed on a Büchi Reveleris® X2 flash chromatography system on Büchi EcoFlex silica columns (4 - 40 g, 40−63 μM, 60 Å). HPLC purifications were conducted with a JASCO HPLC system consisting of PU-4086 Binary semi-preparative pump and UV-4070 UV-vis detector. Compounds were purified with a reversed phase column (COSMOSIL $5C_{18}$-MS-II, 20ID*150 mm) using a linear gradient (from 5% to 40% for 45 min) of acetonitrile in 0.1% aqueous AcOH at a flow rate of 10 mL/min. The effluent was monitored at 254 nm.

Compound characterization. Nuclear magnetic resonance spectroscopy (NMR) was carried out using an Agilent Technologies 400-MR (400/54 Premium Shielded) spectrometer (400 MHz), or on Varian VXR spectrometers (400 MHz and 500 MHz) and recoded at room temperature (22–24 °C). Chemical shifts are reported in δ[ppm] relative to an internal standard (solvent residual peak). The solvents used are indicated for each spectrum. Coupling constants are reported in Hertz [Hz]. Characterization of the signals: s = singlet, d = doublet, t = triplet, q = quartet, m = multiplet, *b*s = broad singlet, dd = doublet of doublet, dt = doublet of triplet. Integration is directly proportional to the number of the protons. Melting point ranges were determined on a Stuart analogue capillary melting point SMP11 apparatus. High Resolution Mass spectra (HRMS) were recorded on an AEI MS-902 mass spectrometer in positive (ESI) mode.

1.2. Synthetic Procedures and NMR Spectra

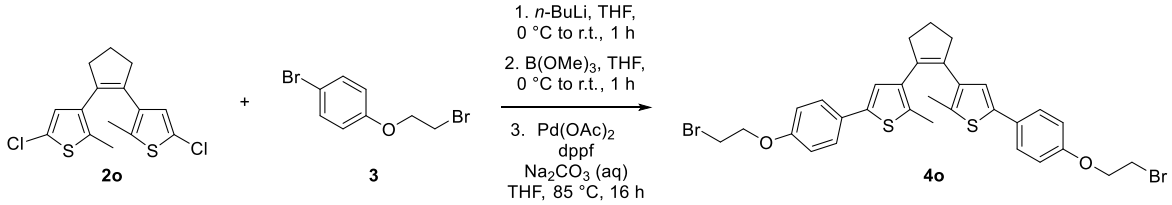

Scheme S1. Synthesis of 1,2-bis(5-(4-(2-bromoethoxy)phenyl)-2-methylthiophen-3-yl)cyclopent-1-ene **4o**.

1,2-Bis(5-chloro-2-methylthiophen-3-yl)cyclopent-1-ene (**2o**)

Compound **2o** was synthesized following a protocol developed earlier by our group.[1]

The identity of the compound was confirmed by ^{1}H-NMR spectroscopy.

^{1}H NMR (400 MHz, $CDCl_3$) δ = 6.57 (s, 2H), 2.71 (t, *J* = 7.5 Hz, 4H), 2.01 (p, *J* = 7.5 Hz, 2H), 1.88 (s, 6H).

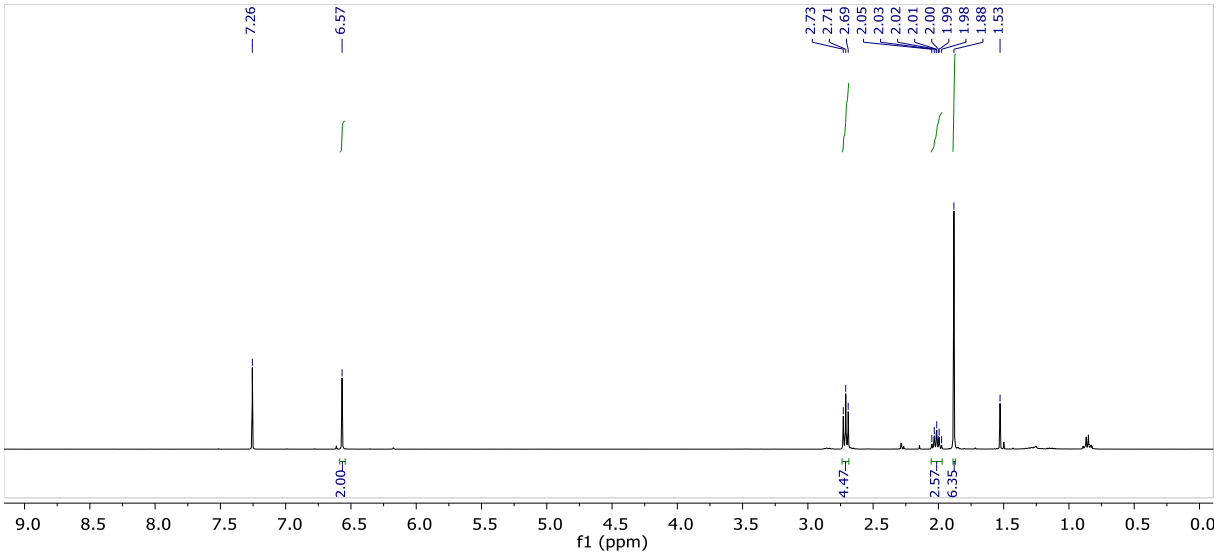

Figure S1. ^{1}H-NMR of **2o** in $CDCl_3$.

1-bromo-4-(2-bromoethoxy)benzene (**2**)

To a solution of NaOH (3.7 g, 92.5 mmol) water (170 mL), 4-bromophenol (10 g, 57.8 mmol) and 1,2-dibromoethane (15 mL, 173.2 mmol) were added and the reaction mixture was stirred at 100 °C for 30 h. Then organic phase was separated, and the aqueous layer extracted with CH_2Cl_2 (3 x 50 mL). The combined organic layers were dried over $MgSO_4$, filtered, and the volatiles were removed *in vacuo*. The crude material was purified by automated flash column chromatography (SiO_2, 20%→50% CH_2Cl_2 in pentane) to obtain the title compound as a colourless, crystalline solid (14.40, 51.4 mmol, 89%). Mp. <50 °C. ^{1}H NMR (400 MHz, Chloroform-*d*) δ = 7.38 (AA'BB', 2H), 6.79 (AA'BB', 2H), 4.25 (t, *J* = 6.2 Hz, 2H), 3.62 (t, *J* = 6.2 Hz, 2H). ^{13}C NMR (101 MHz, Chloroform-*d*) δ = 157.2, 132.4, 116.6, 113.7, 68.1, 28.9.

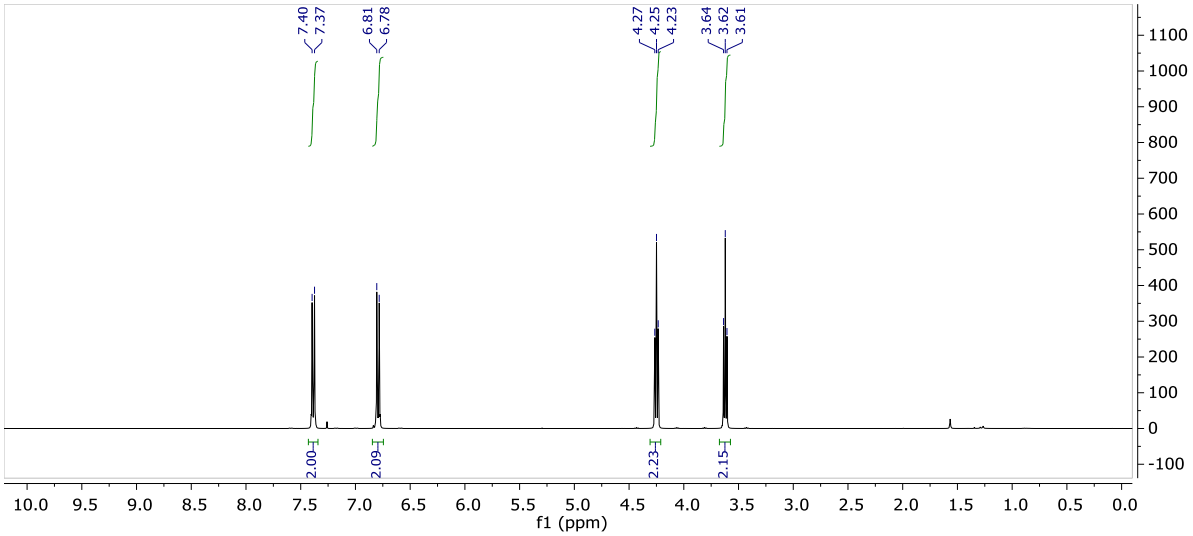

Figure S2. ^{1}H-NMR of **3** in $CDCl_3$.

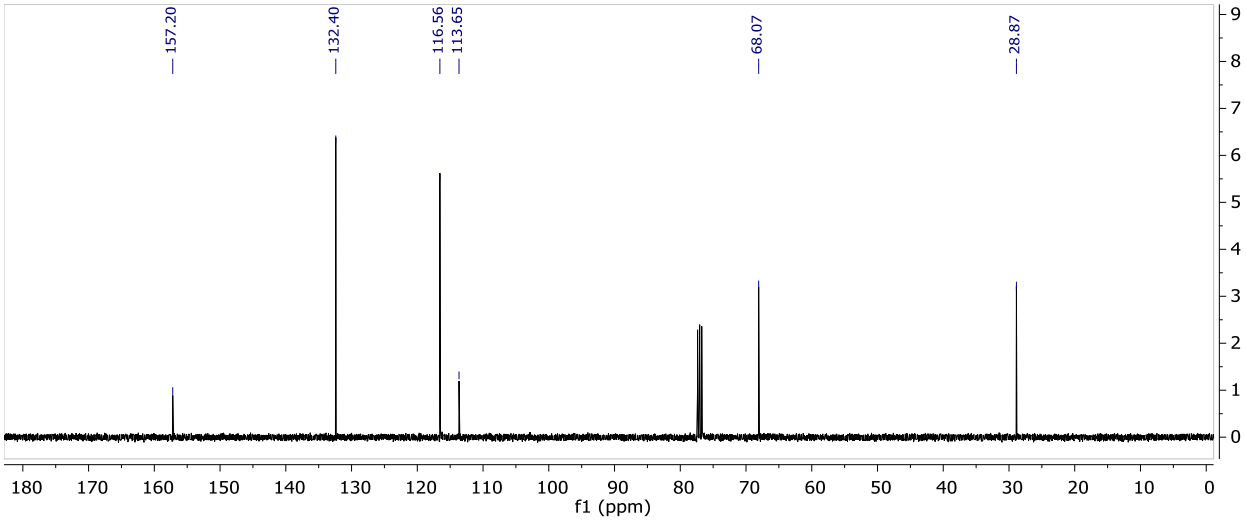

Figure S3. ^{13}C-NMR of **3** in $CDCl_3$.

1,2-bis(5-(4-(2-bromoethoxy)phenyl)-2-methylthiophen-3-yl)cyclopent-1-ene (**4o**)

1,2-Bis(5-chloro-2-methylthiophen-3-yl)cyclopent-1-ene (660 mg, 2.0 mmol) was dissolved in anhydrous THF (24 mL) under nitrogen atmosphere, and *t*-BuLi (2.6 ml 1.7 M in hexane, 4.4 mmol) was added slowly at 0 °C. The reaction mixture was allowed to warm to r.t. and stirred for 1 h. Then, the reaction mixture was cooled again to 0 °C and $B(OMe)_3$ (0.56 mL, 5.0 mmol) was added, followed by stirring for 1 additional hour at ambient temperature. Then, Na_2CO_3 (aq, 2 M, 5 mL) was added and the reaction mixture was deoxygenated by bubbling with nitrogen for 10 min. Subsequently, $Pd(OAc)_2$ (45 mg, 0.20 mmol), dppf (112 mg, 0.20 mmol), and 1-bromo-4-(2-bromoethoxy)benzene (1.12 g, 4.0 mmol) were added and the mixture was heated to 85 °C for 16 h. The reaction mixture was cooled to ambient temperature and diluted with water (50 mL) and EtO_2 (50 mL). The phases were separated, and the aqueous phase was extracted with Et_2O (2 x 50 ml). The combined extracts were dried over Na_2SO_4, filtered, and the solvents evaporated. Purification of the residue by automated flash column

chromatography (SiO2, 5%EtOAc in pentane) gave the title compound as a colourless solid (606 mg, 0.92 mmol, 46% yield). Mp. 101-103 °C. ^{1}H NMR (400 MHz, $CDCl_3$) δ = 7.43 (d, *J* = 8.3 Hz, 4H), 6.94 (s, 2H), 6.89 (d, *J* = 8.5 Hz, 4H), 4.29 (t, *J* = 6.3 Hz, 4H), 3.64 (t, *J* = 6.3 Hz, 4H), 2.85 (t, *J* = 7.3 Hz, 4H), 2.14-2.04 (m, 2H), 2.00 (s, 6H). ^{13}C NMR (101 MHz, $CDCl_3$) δ = 157.3, 139.2, 136.6, 134.6, 133.7, 128.2, 126.6, 123.2, 115.1, 68.0, 38.5, 29.1, 23.0, 14.4. HRMS-ESI^{+} *m/z* calcd for $C_{31}H_{31}Br_2O_2S_2$, $[M+H]^{+}$ 659.0112, found 659.0071.

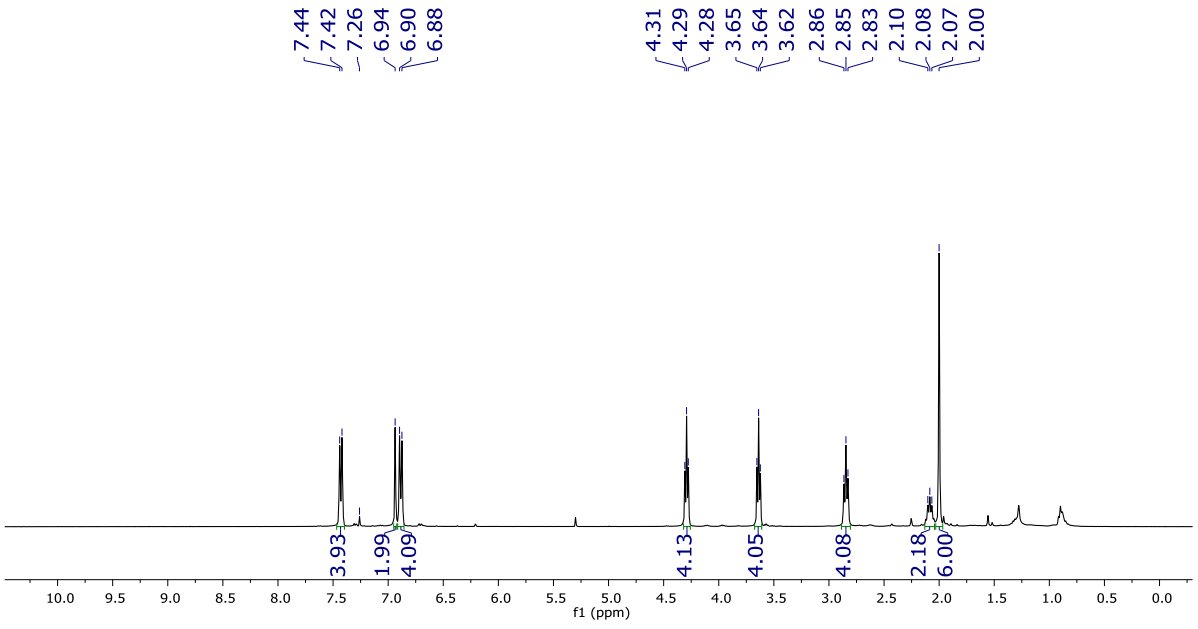

Figure S4. ^{1}H-NMR of **4o** in $CDCl_3$.

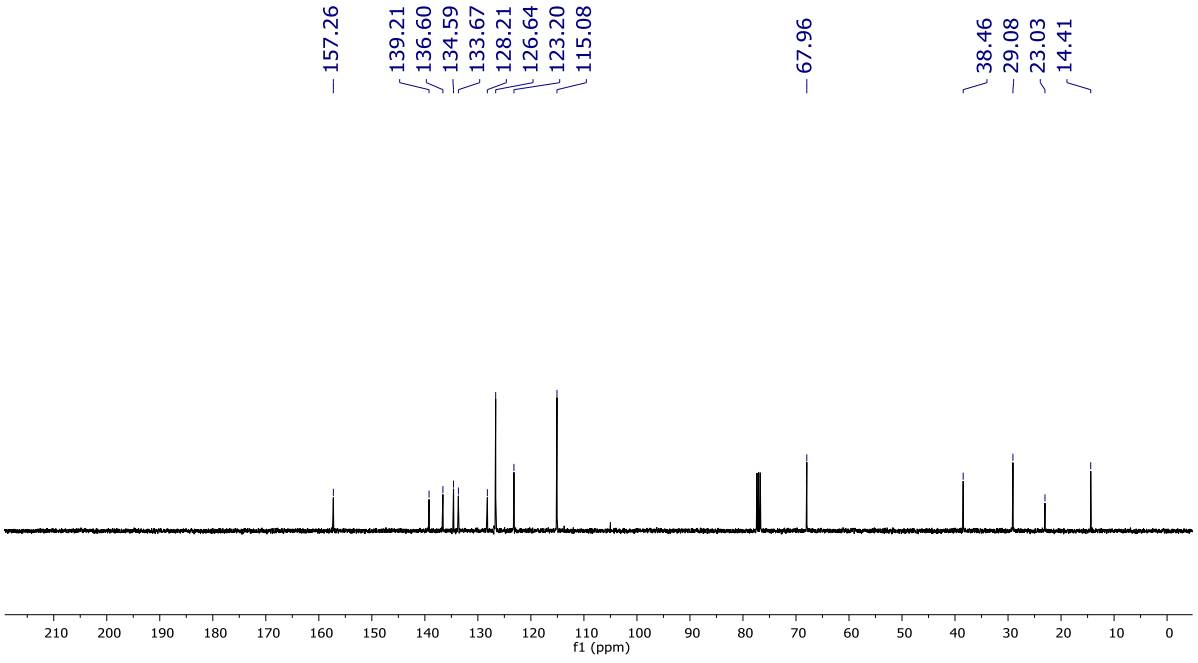

Figure S5. ^{13}C-NMR of **4o** in $CDCl_3$.

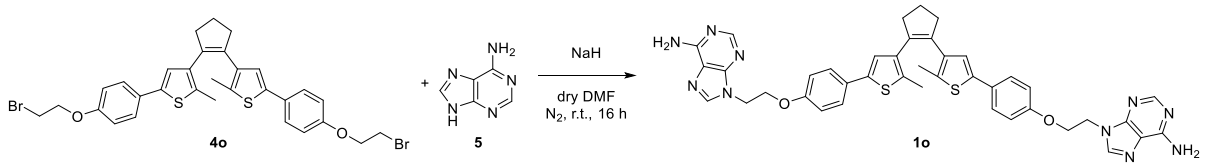

Scheme S2. Synthesis of 9,9'-((((4,4'-(cyclopent-1-ene-1,2-diyl)bis(5-methylthiophene-4,2-diyl))bis(4,1-phenylene))bis(oxy))bis(ethane-2,1-diyl))bis(9H-purin-6-amine) **1o**.

9,9'-((((4,4'-(cyclopent-1-ene-1,2-diyl)bis(5-methylthiophene-4,2-diyl))bis(4,1-phenylene))bis-(oxy))bis(ethane-2,1-diyl))bis(9H-purin-6-amine) (**1o**)

A mixture of adenine (82.1 mg, 0.6 mmol) and NaH (24.3 mg, 60% in mineral oil, 0.6 mmol) in anhydrous DMF was stirred under nitrogen atmosphere for 2 h, until a white precipitate was formed. Then dibromoalkyl switch **4o** (200 mg, 0.30 mmol) was added and reaction mixture was stirred at room temperature for 16 h. The solvent was evaporated, and the product was recrystallized in EtOH/H_2O to give **1o** as a white solid (120 mg, 0.16 mmol, 52%). Mp 163-165 °C. ^{1}H NMR (500 MHz, DMSO-d_6) δ = 8.17 (s, 2H), 8.15 (s, 2H), 7.41 (d, J = 8.4 Hz, 4H), 7.22 (s, -NH_2, 4H), 7.11 (s, 2H), 6.92 (d, J = 8.5 Hz, 4H), 4.52 (m, 4H), 4.37 (m, 4H), 2.80 (m, 4H), 2.01 (m, 2H), 1.89 (s, 6H). ^{13}C NMR (101 MHz, DMSO-*d6*) δ = 157.7, 156.4, 152.9, 150.0, 141.6, 139.1, 137.0, 134.5, 132.9, 127.4, 126.6, 123.7, 119.1, 115.5, 66.2, 42.9, 38.4, 22.7, 14.4. HRMS-ESI$^+$ *m/z* calcd for $C_{41}H_{39}N_{10}O_2S_2$, $[M+H]^+$ 767.2653, found 767.2693.

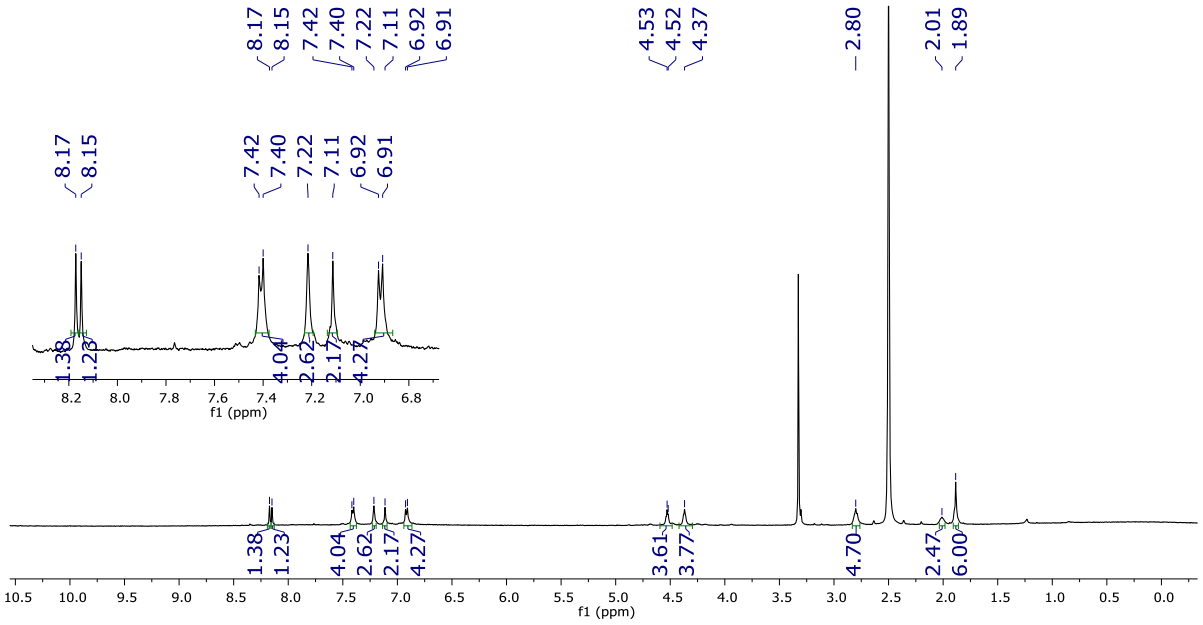

Figure S6. ^{1}H-NMR of **1o** in DMSO-d_6.

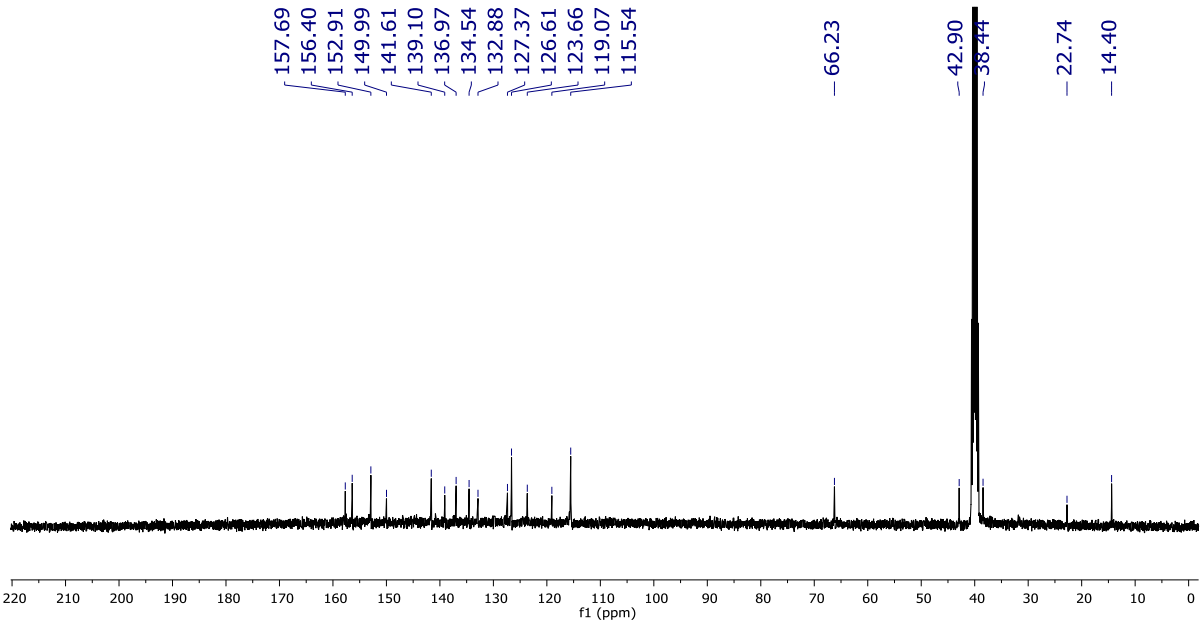

Figure S7. ^{13}C-NMR of **1o** in DMSO-d_6.

2. Photophysical Characterization and Photochemical Isomerization by UV-Vis and NMR Spectroscopy

UV/Vis absorption spectra were recorded on a JASCO V630 spectrophotometer and on an Agilent 8453 UV-Visible Spectrophotometer. Photochemical isomerization was achieved by irradiation from the side in a fluorescence quartz cuvette (width = 1.0 cm) using a 300 nm LED (M300F2, Thor Labs) or irradiated through a 420 nm cut-off filter with a microscope lamp equipped with a fiber optic. A Quantum Northwest TC1 temperature controller was used to maintain the temperature at 20 °C during photochemical studies. Raw data were processed using Agilent UV-Vis ChemStation B.02.01 SP1, Spectra Manager, Spectragryph 1.2, and OriginPro 2016.
For photostationary distribution (PSD) determination by ^{1}H NMR 0.7 mL of a 1 mM solution of the respective compound in DMSO-*d6* was irradiated in a fluorescence quartz cuvette (width = 1.0 cm) using a using a 300 nm LED (M300F2, Thor Labs) and transferring the solution in a NMR tube subsequently.

2.1.Extinction coefficient of **1o** in EtOH

The extinction coefficients were calculated by preparing solutions of **1o** in EtOH containing a known concentration. The most concentrated solution was subsequently diluted, and the absorption spectra of each solution were recorded.

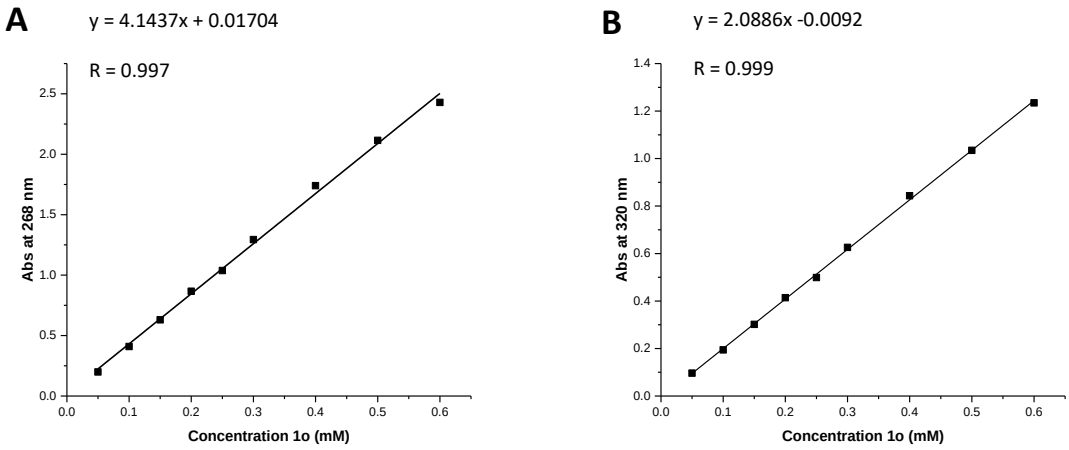

Figure S8. Molar attenuation coefficient of **1o** in EtOH by UV-Vis spectroscopy in EtOH at (**A**) 268 nm and (**B**) 320 nm to give ε(268 nm) = 41437 L mol^{-1}cm^{-1} and ε(320 nm) = 20886 L mol^{-1}cm^{-1}, respectively.

2.2.UV-Vis Spectra of the Photoisomerization of **1**

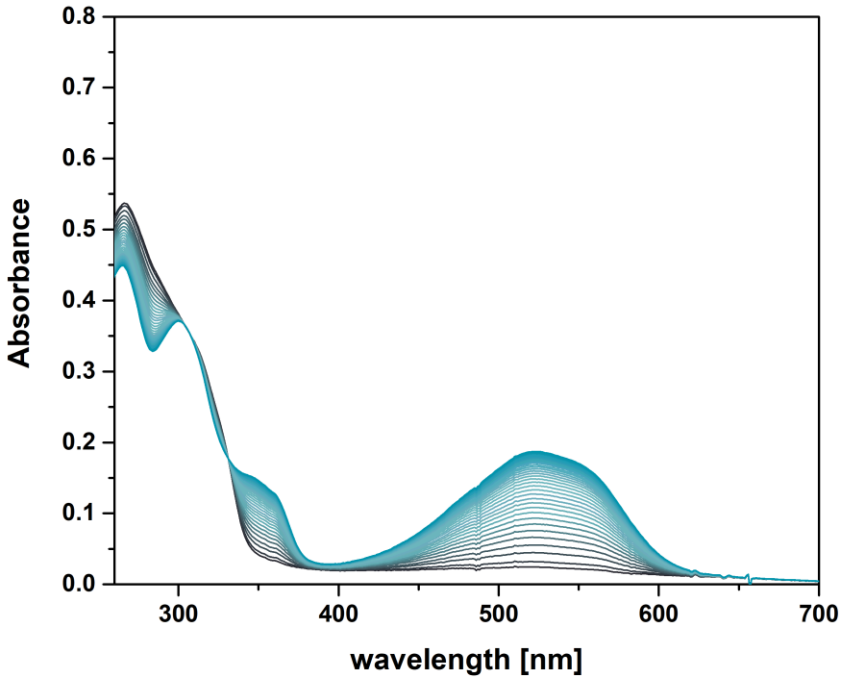

Figure S9. Time-resolved UV-Vis absorption spectrum of DTE **1** (10 µM) in EtOH:TE buffer 1:1 while irradiating with a 300 nm LED.

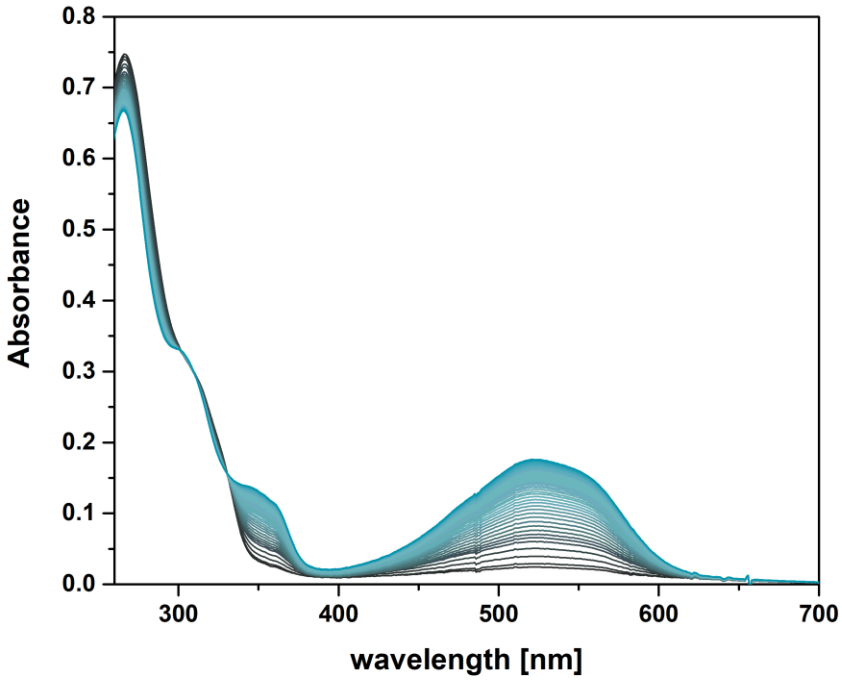

Figure S10. Time-resolved UV-Vis absorption spectrum of DTE **1** (10 µM) and dT_{20} (2 µM) in EtOH:TE buffer 1:1 while irradiating with a 300 nm LED.

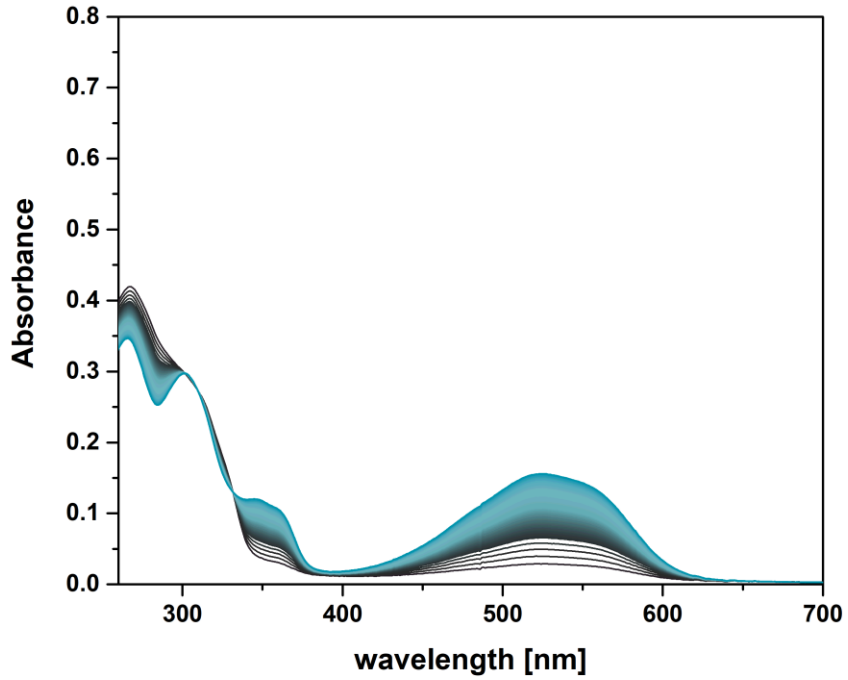

Figure S11. Time-resolved UV-Vis absorption spectrum of DTE **1** (10 µM) in EtOH while irradiating with a 300 nm LED.

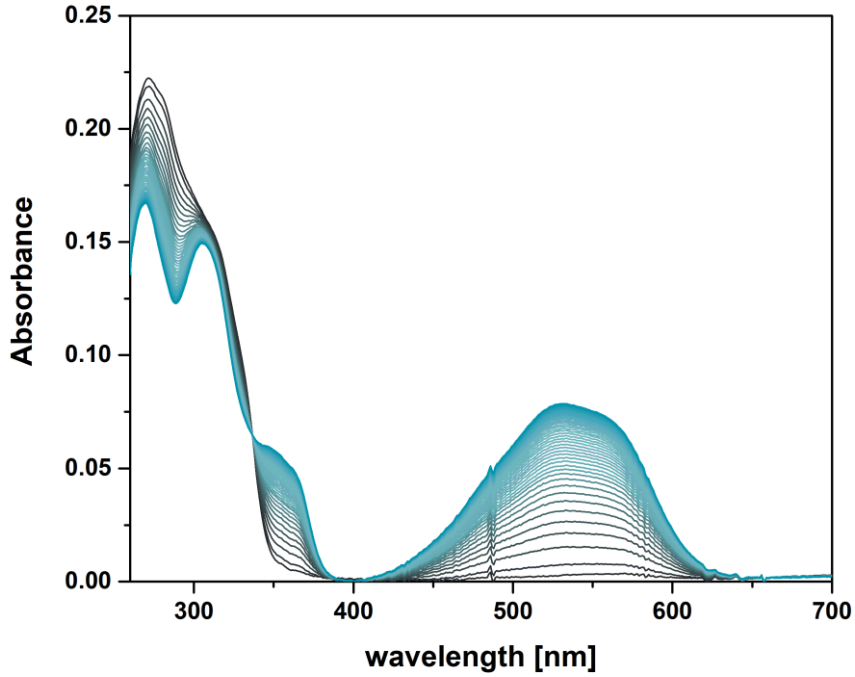

Figure S12. Time-resolved UV-Vis absorption spectrum of DTE **1** (5 µM) in DMSO while irradiating with a 300 nm LED.

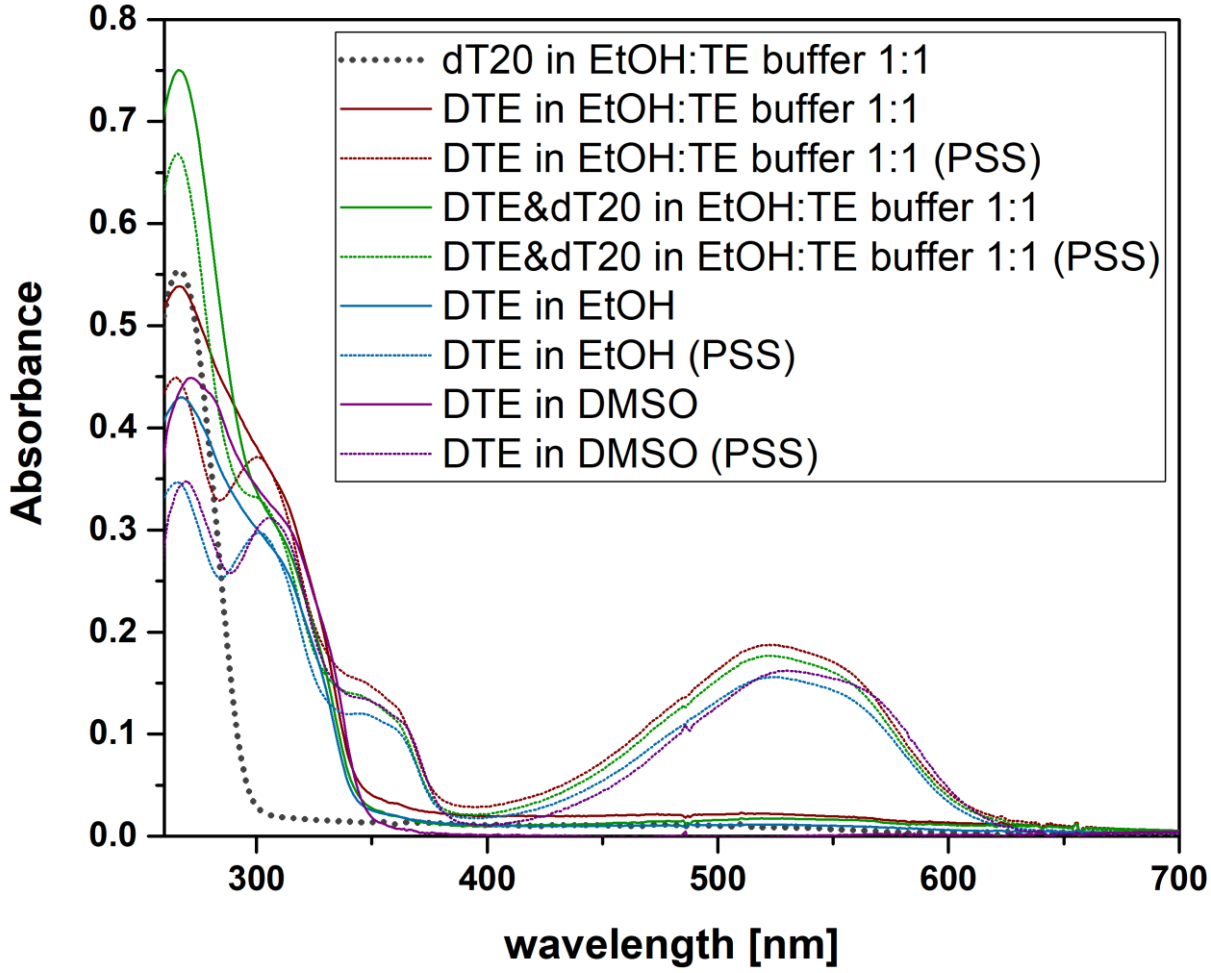

Figure S13. UV-Vis absorption spectra of DTE **1** (10 μM) in different solvents before irradiation and at the PSS^{300}.

2.3.PSD Determination by ^{1}H-NMR

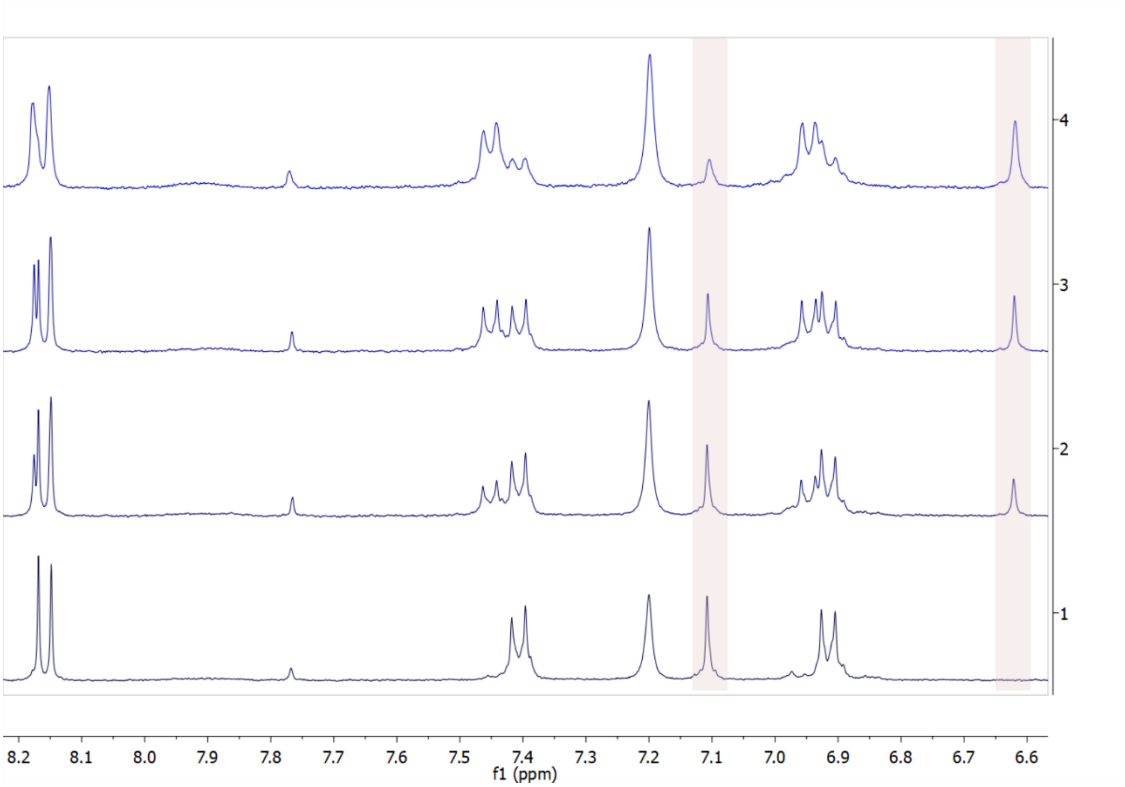

Figure S14. Irradiation of a 1 mM solution of DTE **1** in DMSO-*d6* (ca. 700 µL in a 10x10 mm fluorescence quartz cuvette) using a 300 nm LED. Aromatic region of the ^{1}H spectrum of DTE **1**; bottom to top: 0 min, 4 min, 8 min, 15 min (=PSS). Highlights show the characteristic thiophene singlet at 7.1 ppm (open) or 6.6 ppm (closed isomer), respectively.

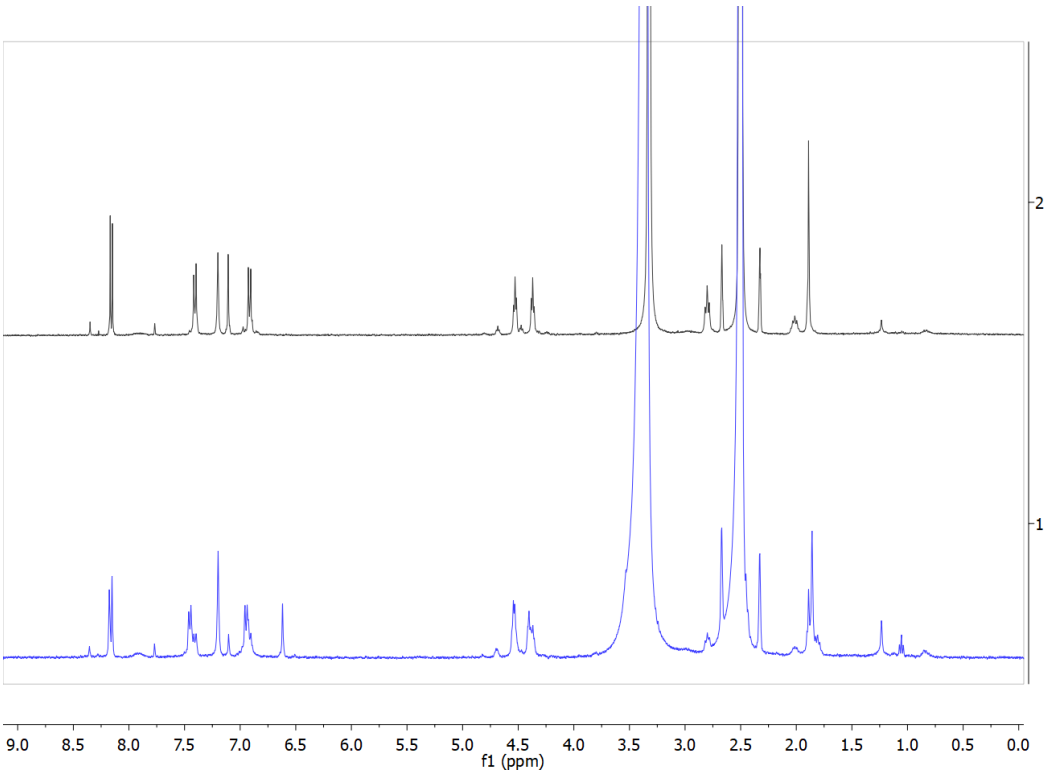

Figure S15. Full ^{1}H spectrum of DTE **1** in DMSO-*d6* before (top) and after (bottom) irradiation.

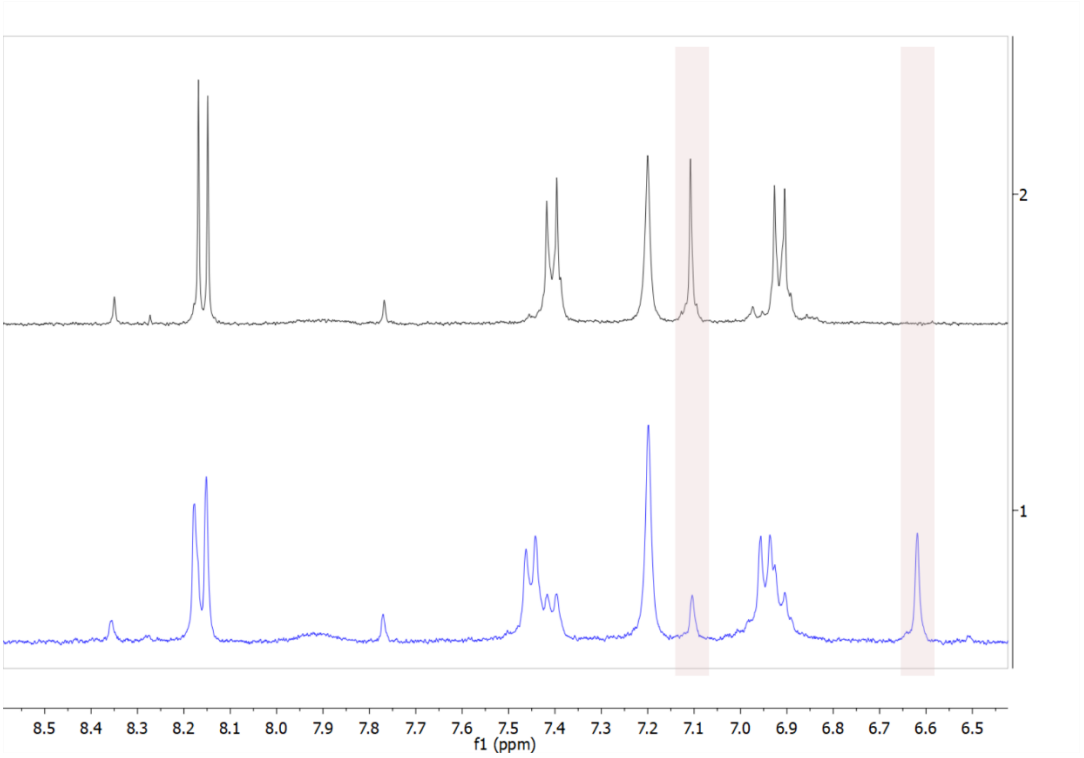

Figure S16. Aromatic region of the ^{1}H spectrum of DTE **1** in DMSO-*d6* before (top) and after (bottom) irradiation. Highlights show the characteristic thiophene singlet at 7.1 ppm (open) or 6.6 ppm (closed isomer), respectively.

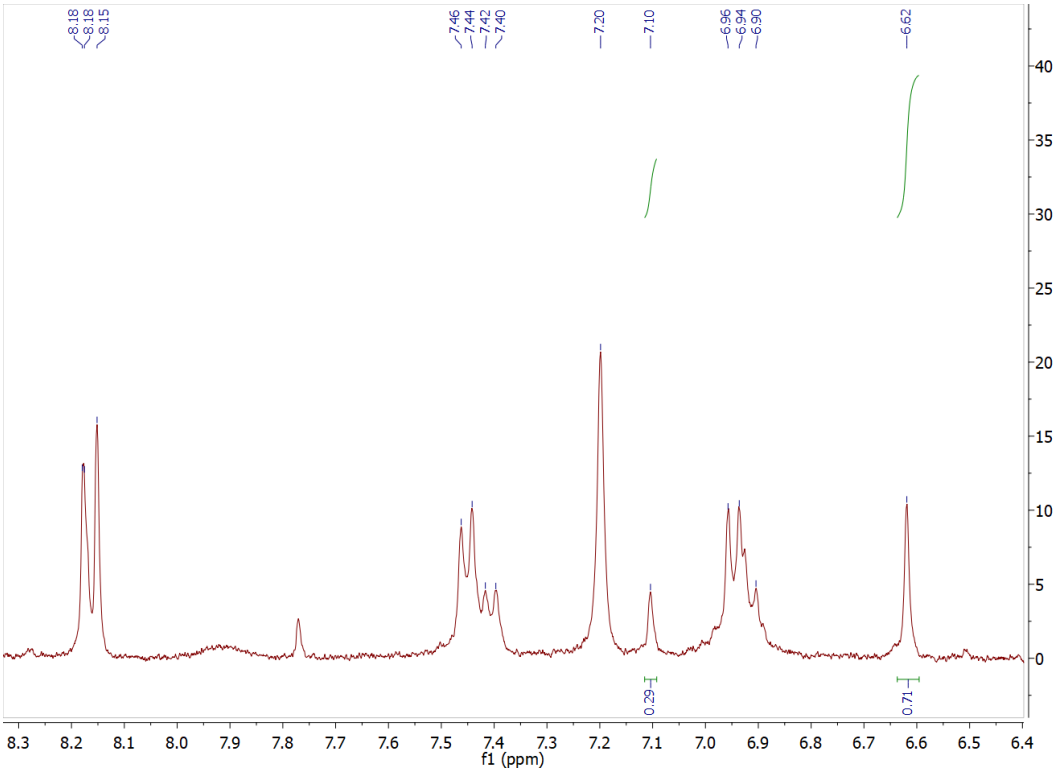

Figure S17. Aromatic region of the ^{1}H spectrum of DTE **1** in DMSO-*d6* at the PSS^{300} with integration of characteristic thiophene singlet at 7.1 ppm (open) or 6.6 ppm (closed isomer), respectively, to assign a PSD^{300} of 71:29 *C*:*O*.

3. Formation of Supramolecular Assemblies: Sample Preparation

Stock solutions of DTE **1o** (0.55 mM, EtOH) and **dT$_{20}$** (55 µM, TE buffer) were prepared. Both stock solutions were mixed as specified with the individual experiment in a HPLC vial (1.5 mL, crimp top) to give a colourless suspension, and sealed airtight. Typically, a 1:1 mixture of both stock solution (150 µL each) was used to give a final solution of **1o** (0.25 mM) and **dT$_{20}$** (25 µM) in EtOH:TE buffer 1:1 (300 µL) and a base pair ratio of 1:1 (A:T). This combination was chosen as it showed on the microscopic (TEM, *vide infra*) and macroscopic scale the most promising results after optimization.

The solutions were sonicated at 75 °C for *ca*. 90 min and became clear (Figure S18A). Already after a few moments outside of the bath, the solutions started to become turbid again (Figure S18B) and were further cooled on ice for 60 min and then placed in the fridge for *ca*. 18 h. The aging process was continued at room temperature for at least 7 d. The samples were kept in the dark.

For irradiation, a 300 nm LED (M300F2, Thor Labs) or a 526 nm LED (Sahlmann cooled 3 x LXML PM01 0100, 526 nm, FWHM = 35.1 nm, power output = 810 mW) were used. Irradiation with 300 nm light was done through the open top of the vials to avoid filtering by the glass of the vial. Figure S18C shows irradiated samples after sonication.

Figure S18. Sample preparation. **A**. **1o** and **dT$_{20}$** after sonication. **B**. **1o** and **dT$_{20}$** after a few minutes at ambient temperature. **C**. **1c** (PSS^{300}) and **dT$_{20}$** after sonication.

4. Circular Dichroism (CD) Spectroscopy

Circular dichroism (CD) spectra were recorded on JASCO J815 CD spectrometer equipped with a Peltier temperature controller. Measurements were performed in a quartz cuvette (width = 1 mm) at -5 °C unless otherwise stated. Irradiation was performed outside of the spectrometer with a suitable light source in a distance of *ca*. 0.5 cm. For irradiation, a 300 nm LED (M300F2, Thor Labs) or a 526 nm LED (Sahlmann cooled 3 x LXML PM01 0100, 526 nm, FWHM = 35.1 nm, power output = 810 mW) were used.

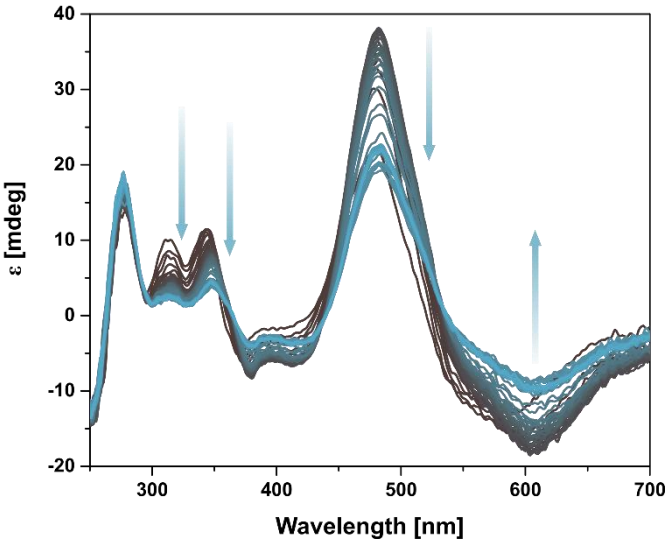

Figure S19. Time-resolved CD spectrum of **1c** and **dT$_{20}$** (1:1, at the PSS^{300}, EtOH:TE buffer 1:1) showing the evolution of the spectra over two days (grey to blue solid lines, 60 min intervals, kept at 0 °C).

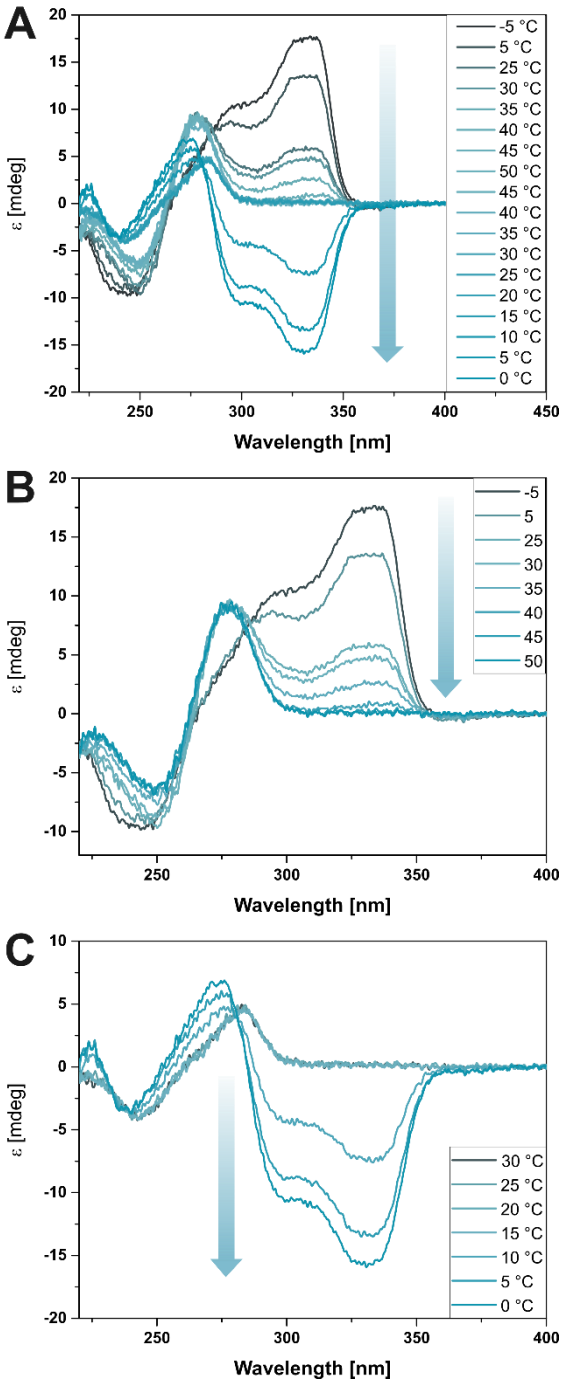

Figure S20. VT-CD spectra showing the reversibility of the system. **A**. Full heating-cooling cycle showing the melting of DNA hybrid assembly and the regeneration of the kinetic state. **B**. Melting of the DNA-hybrid. **C**. Self-assembly of the dissociated components upon cooling.

5. Transmission Electron Microscopy (TEM)

Three microliter of each sample were pipetted onto a glow-discharged plain carbon coated 400 mesh copper grid and was negatively stained with 2% uranyl acetate. TEM images were recorded on a Philips CM120 electron microscope (FEI, Eindhoven, the Netherlands) equipped with a LaB_6 cathode, operated at 120 kV and a Philips CM12 electron microscope (FEI, Eindhoven, the Netherlands) equipped with a tungsten filament, operated at 120 kV.

For irradiation, a 300 nm LED (M300F2, Thor Labs) or a 526 nm LED (Sahlmann cooled 3 x LXML PM01 0100, 526 nm, FWHM = 35.1 nm, power output = 810 mW) were used. Irradiation with 300 nm light was done through the open top of the vials to avoid filtering by the glass of the vial.

5.1. Screening of different Base Pair Ratios

To find the best condition to form a molecular recognition-driven self-assembly, we screened different ratios of adenine-functionalized DTE and thymine-based ssDNA.

Table S1. Pipetting scheme of stock solutions of DTE **1o** (0.55 mM, EtOH) and **dT_{20}** (55 µM, TE buffer) and corresponding ratio of adenine (A) and thymine (T) units.

Entry	DTE [µL]	DNA [µL]	Adenine Units	Thymine Units	A:T Ratio
1	130	170	17.34	22.66	0.76
2	135	165	18.00	22.00	0.82
3	270	330	18.00	22.00	0.82
4	280	320	18.66	21.34	0.88
5	290	310	19.34	20.66	0.94
6	300	300	20.00	20.00	1.00
7	320	280	21.34	18.66	1.14

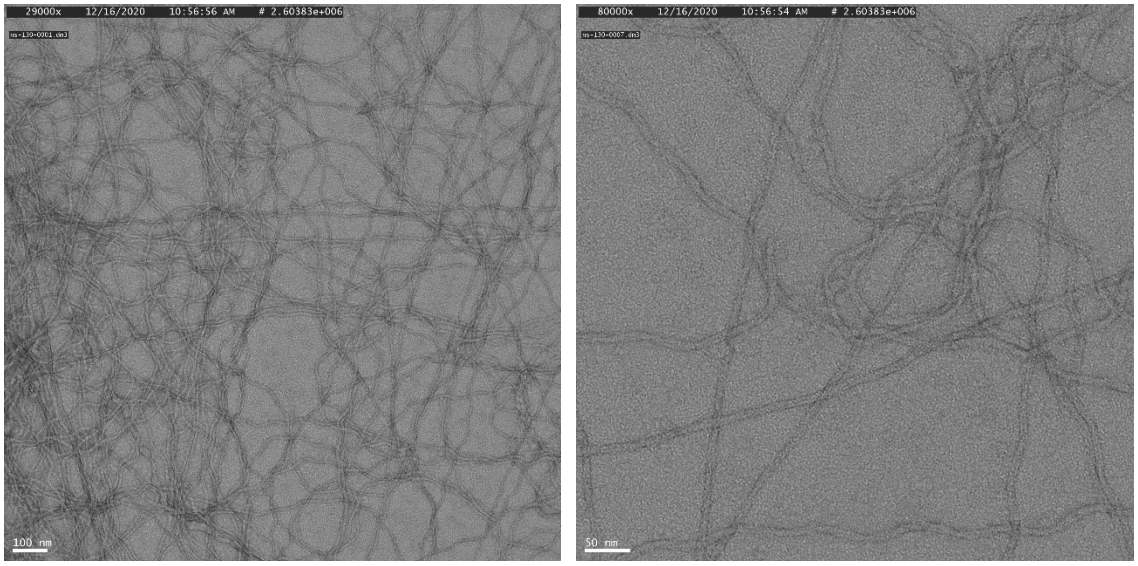

Figure S21. TEM image of the thermodynamic product of **1o** and **dT_{20}** (A:T = 0.76, EtOH:TE buffer = 0.76, 300 µL sample volume for aging).

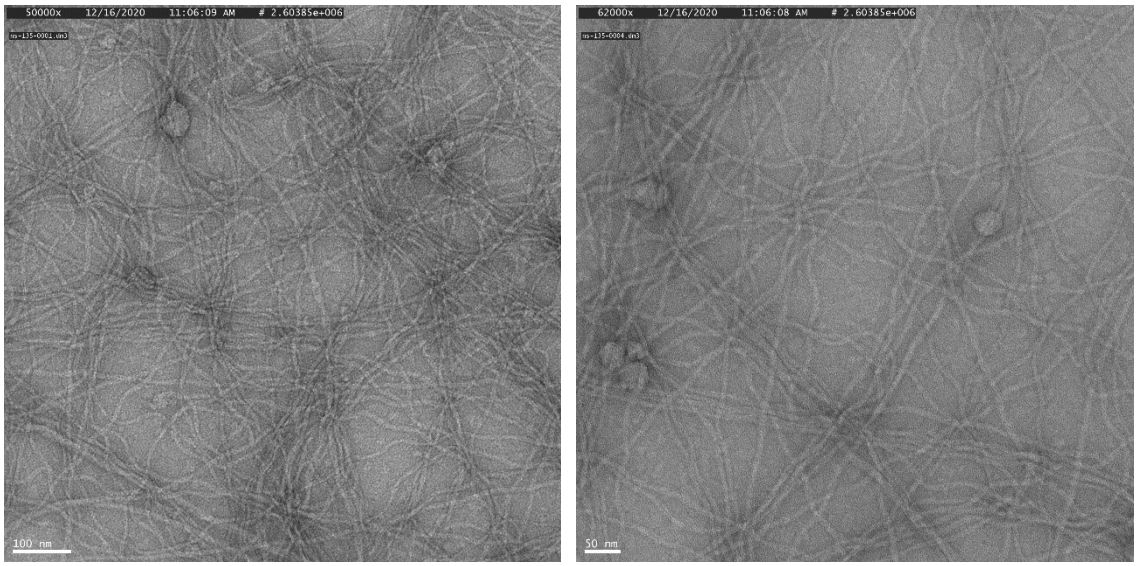

Figure S22. TEM image of the thermodynamic product of **1o** and **dT_{20}** (A:T = 0.82, EtOH:TE buffer = 0.82, 300 µL sample volume for aging).

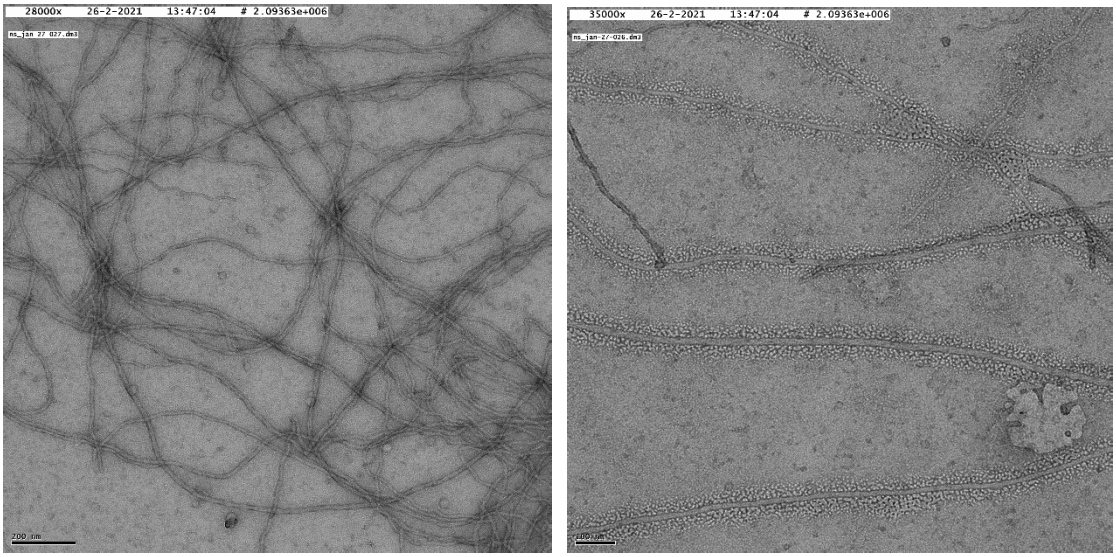

Figure S23. TEM image of the thermodynamic product of **1o** and **dT_{20}** (A:T = 0.82, EtOH:TE buffer = 0.82, 600 µL sample volume for aging).

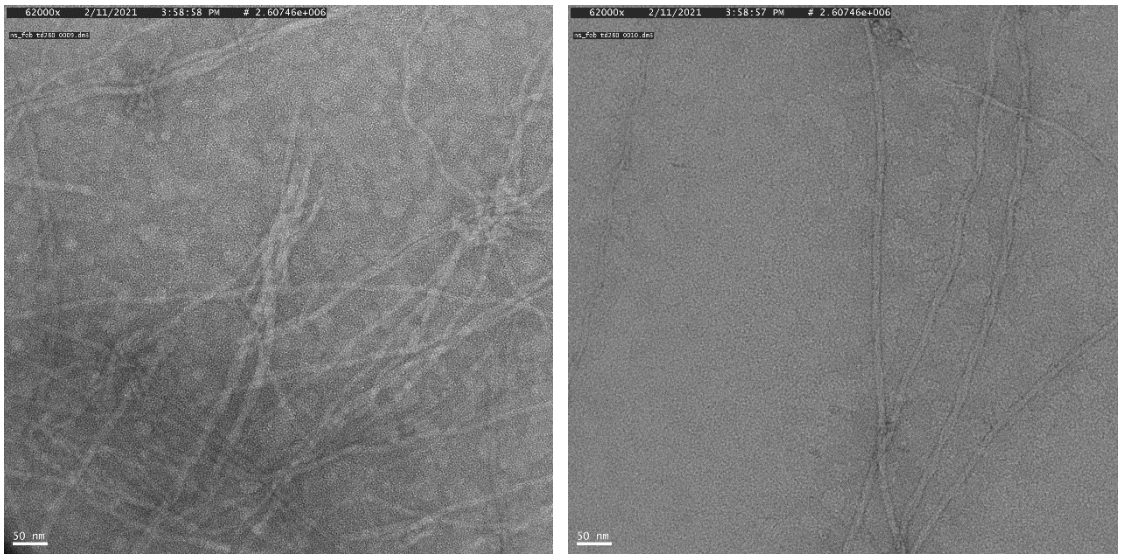

Figure S24. TEM image of the thermodynamic product of **1o** and $\mathbf{dT_{20}}$ (A:T = 0.88, EtOH:TE buffer = 0.88, 600 µL sample volume for aging).

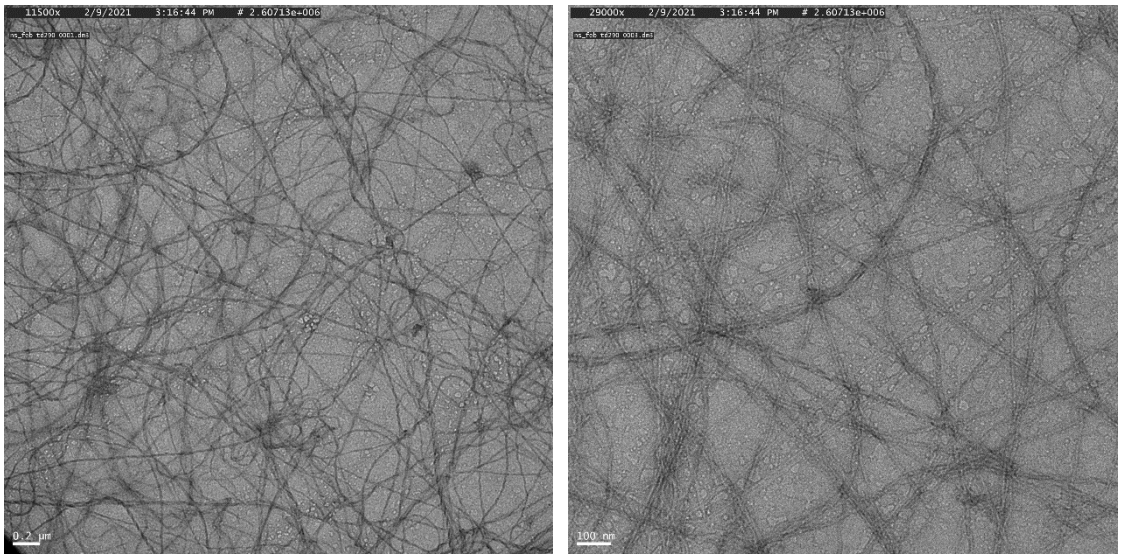

Figure S25. TEM image of the thermodynamic product of **1o** and $\mathbf{dT_{20}}$ (A:T = 0.94, EtOH:TE buffer = 0.94, 600 µL sample volume for aging).

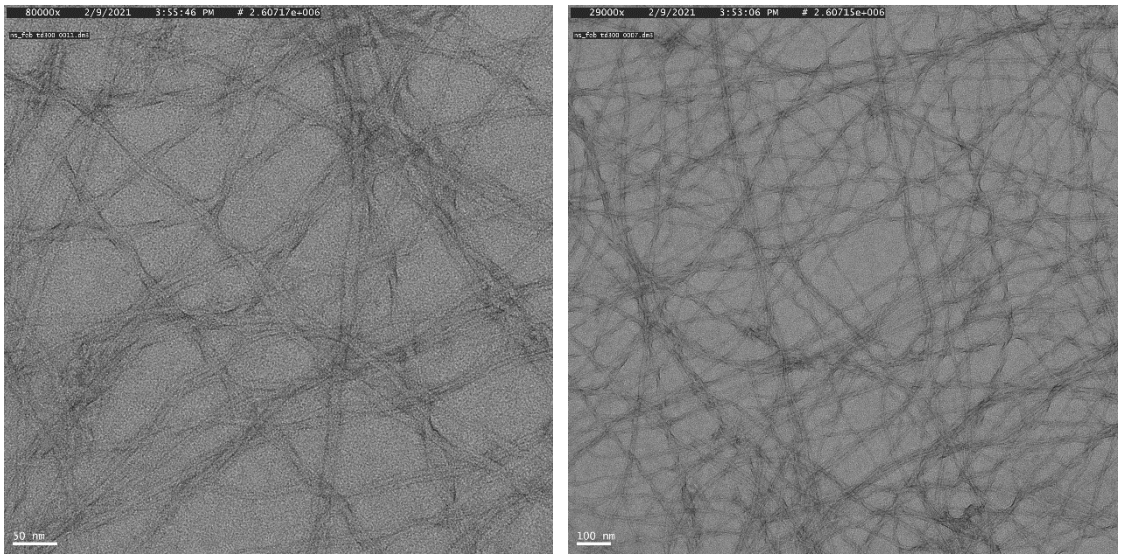

Figure S26. TEM image of the thermodynamic product of **1o** and **dT_{20}** (1:1, EtOH:TE buffer 1:1, 600 µL sample volume for aging).

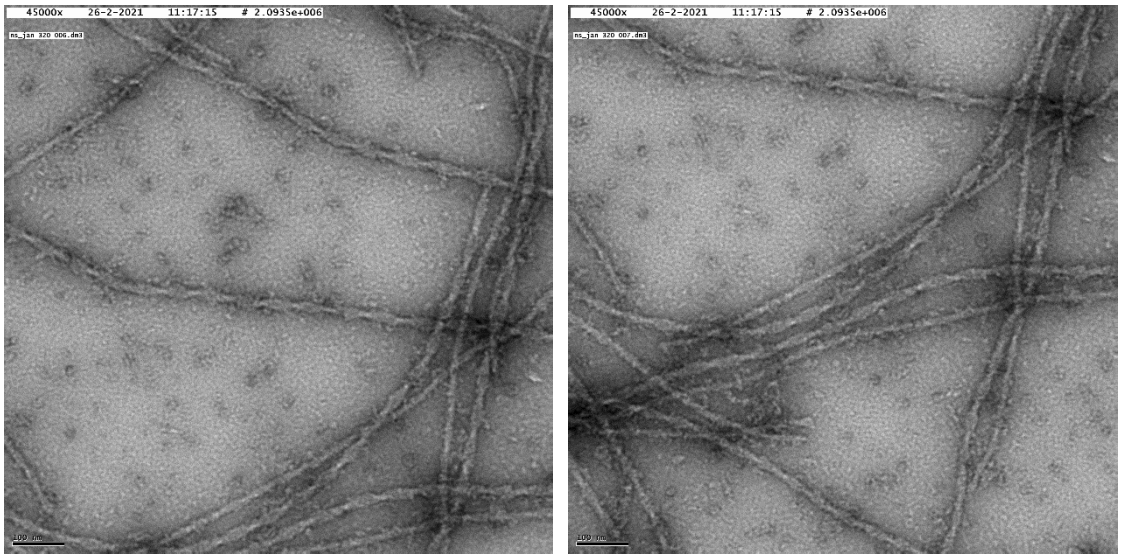

Figure S27. TEM image of the thermodynamic product of **1o** and **dT_{20}** (A:T = 1.14, EtOH:TE buffer = 1.14, 600 µL sample volume for aging).

5.2.Aging Process of **1o** and **dT$_{20}$**

To follow the aging process of a sample of **1o** and **dT$_{20}$** at the microscopic scale, we imaged samples at different time points. The image of the inatally formed metastable aggregates can be found in Figure 3 and 4 the main text.

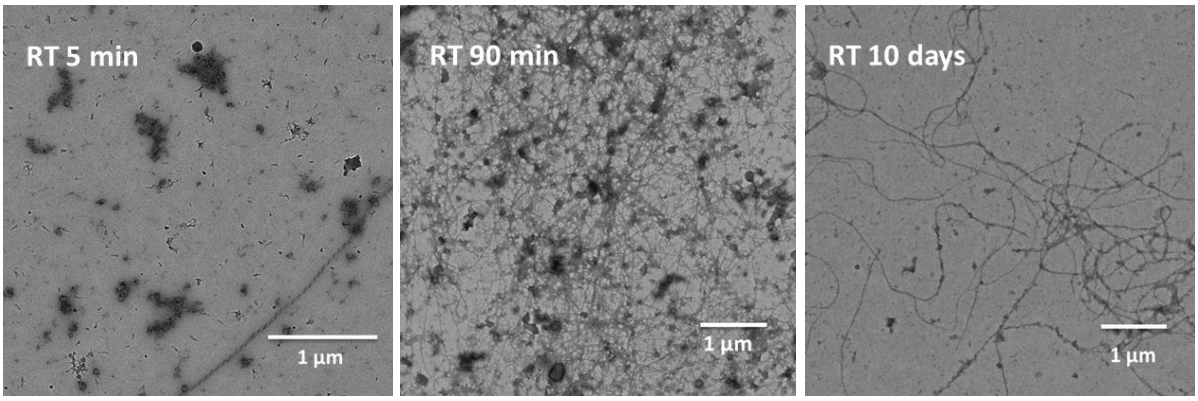

Figure S28. TEM images of the transition from kinetic aggregates to the thermodynamic product of **1o** and **dT$_{20}$** (1:1, EtOH:TE buffer 1:1). The sample was prepared as described in section S3 and stored in the dark at ambient temperature.

5.3.TEM of aged **1c** and **dT$_{20}$**

A sample of **1o** and **dT$_{20}$** was prepared as described in section S3 and aged for 5 days at ambient temperature. Then, the samples was irradiation with 300 nm light to convert **1o** into the *C* isomer (PSD^{300} of 71:29 *C*:*O* in DMSO-*d6, vide supra*). After a heating-cooling cycle, the sample was aged in imaged.

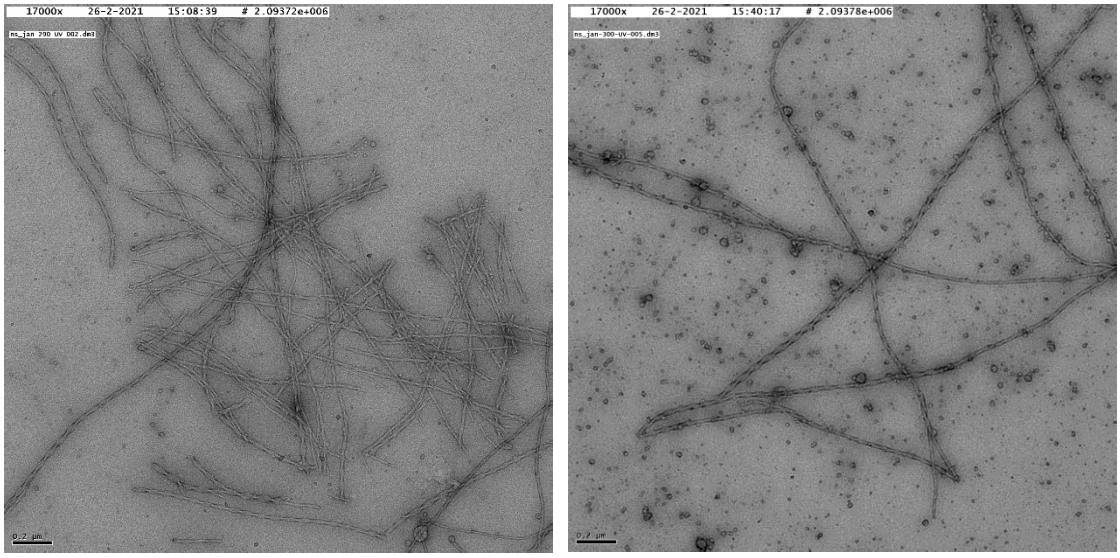

Figure S29. TEM images of the thermodynamic product of **1c** and **dT$_{20}$** (1:1, PSS^{300}, EtOH:TE buffer 1:1).

5.4.TEM of aged **1o** and **dT$_{20}$** after Staining or Irradiation

Hydrogels grown from **1c** and **dT$_{20}$** (1:1, PSS^{300}, EtOH:TE buffer 1:1) were treated with UV light or stained with ethidium bromide and imaged.

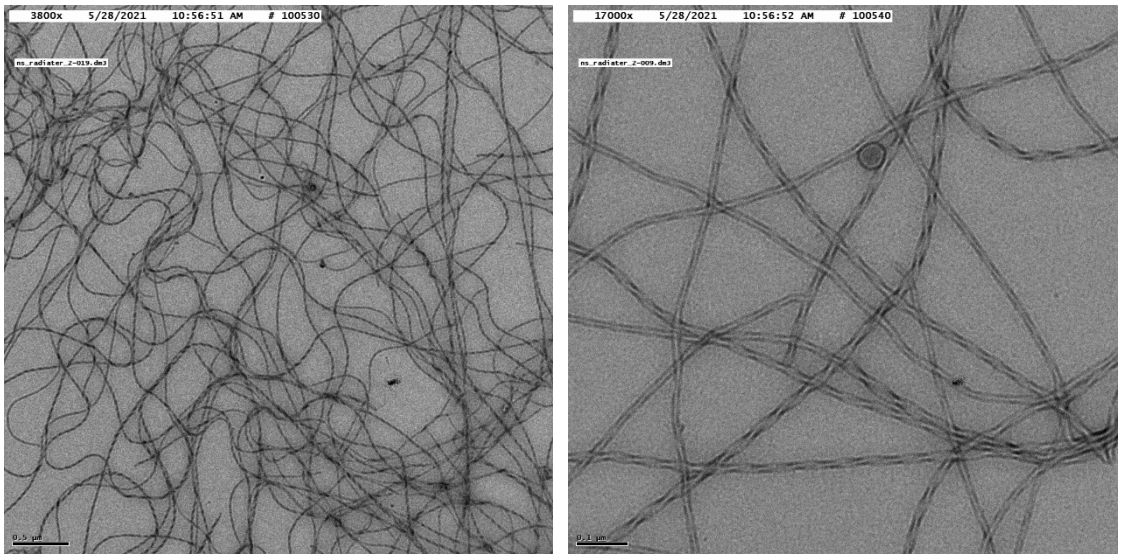

Figure S30. TEM image of a hydrogel grown from **1c** and **dT$_{20}$** (1:1, PSS^{300}, EtOH:TE buffer 1:1) after irradiation with 300 nm light and accompanied light-induced shrinking (*cf*. Figure S47 for the macroscopic image).

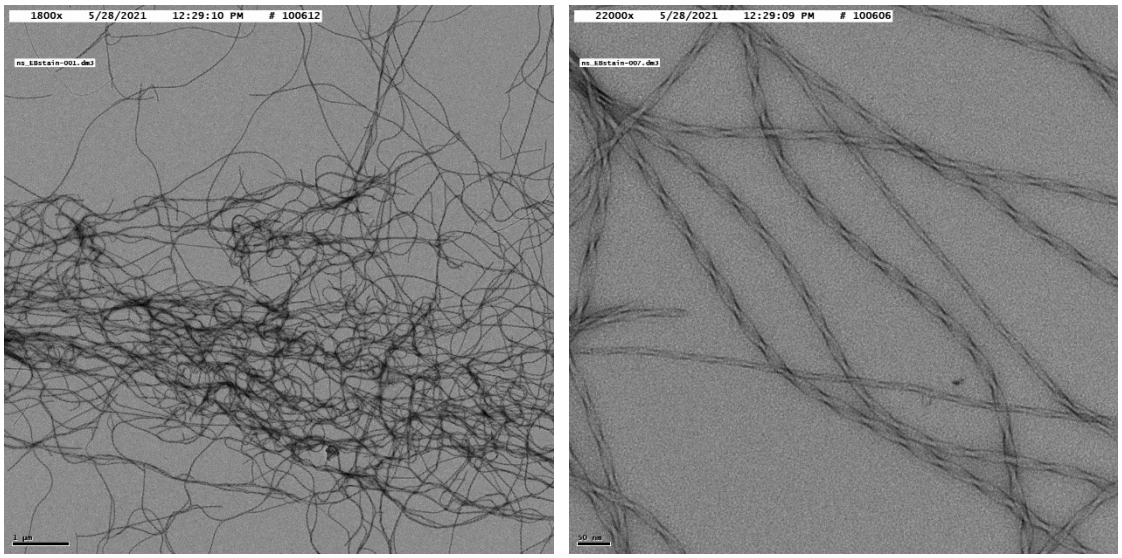

Figure S31. TEM image of a hydrogel grown from **1c** and $\mathbf{dT_{20}}$ (1:1, PSS^{300}, EtOH:TE buffer 1:1) after staining with ethidium bromide (*cf.* fluorescence microscopy images in section S6).

5.5.TEM after Recycling

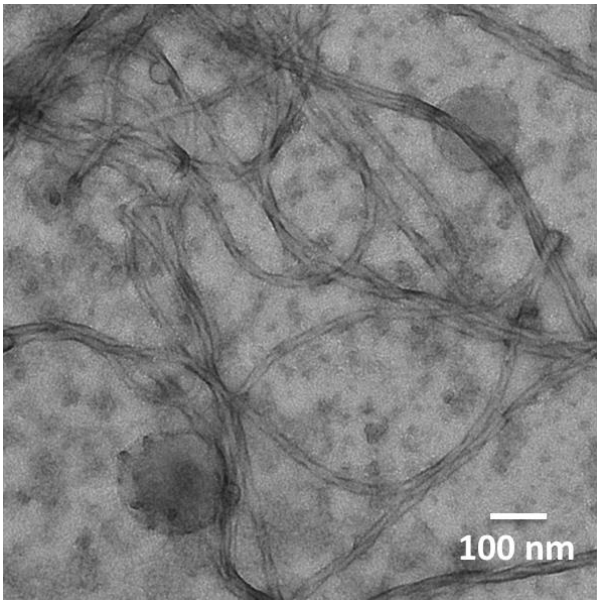

Figure S32. Recyclability. TEM image of a sample of **1c** and $\mathbf{dT_{20}}$ (1:1, EtOH:TE buffer 1:1) after irradiation with visible light followed by a heating-cooling cycle and aging.

6. Atomic Force Microscopy (AFM)

Atomic Force Microscopy (AFM) was performed on a SPM Nanoscope IIIa multimode working on tapping mode with a RTESPA tip (Veeco) at a working frequency of ~235 Khz. Twisted Ribbons could be observed after drying a drop-casted solution of **1o** and **dT_{20}** (1:1, EtOH:TE buffer 1:1), which present a positive ICD, on a mica substrate. Prior to the measurement the concentration of the sample was adjusted by dilution of *ca*. 1/10 to avoid overloading the subtrate. Two exmeplariy measurements are displayed in Figure S33.

The stabilization of the ribbons on polar surfaces also indicates that most probable is the backbone of the DNA which interacts with the substrate and thus **dT_{20}** remains in the periphery of the self-assembled **1o**:**dT_{20}** 1:1 complex. To additionally obtain AFM images in solution was unfortunatelly not succesul for this system.

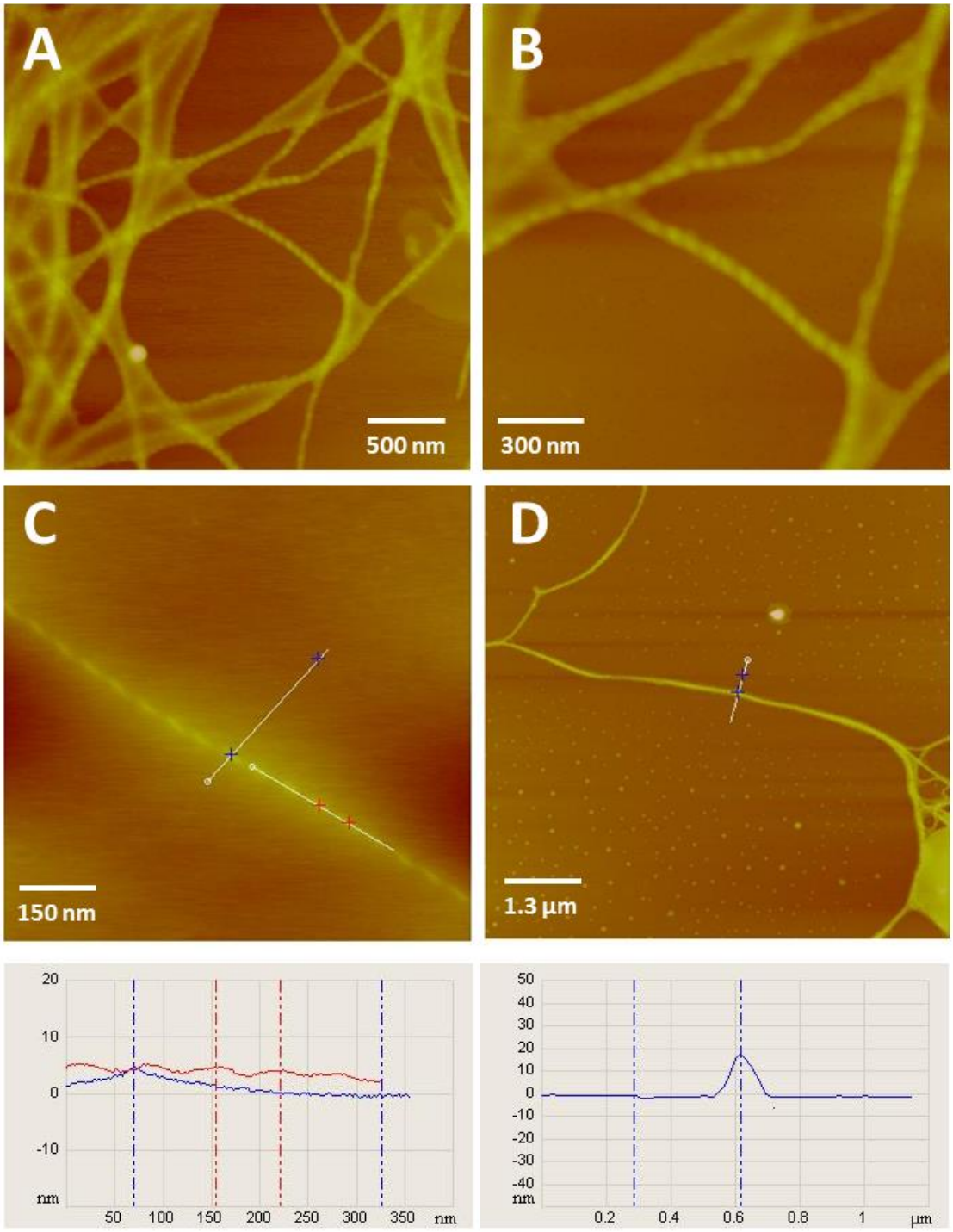

Figure S33A–**D**. AFM images of the thermodynamic product of **1o** and **dT_{20}** (A:T = 1.1, EtOH:TE buffer = 1.1) on surface with **C** and **D** displaying exemplarily measurements of the helical pitch (red in C, 67 nm) and the height (blue in C = 5.2 nm; blue in D = 18.7 nm) of the twisted ribbons on surface.

7. Fluorescence Microscopy

The shape-resilient hydrogels were stained with the DNA intercalator ethidium bromide for fluorescence microscopy. Specifically, the TE buffer solution of a *ca*. three-month aged cylindrically shaped hydrogel was exchanged with a 55 µM solution of ethidium bromide in pure TE buffer. The sample was incubated for three weeks at ambient temperature in a sealed vial.

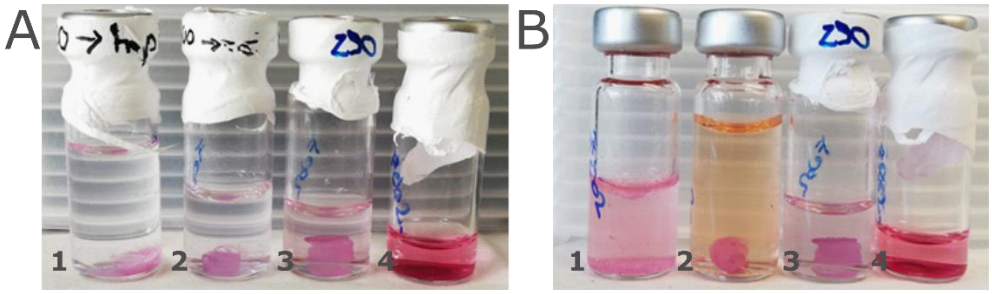

Figure S34. Exchanging the solvent of the hydrogels in vial 1 and 2. Specifically, vial 1 from heptane (**A**) to ethidium bromide (55 µM in TE buffer, **B**) and vial 2 from TE buffer (**A**) to ethidium bromide (55 µM in TE buffer, **B**). Vials 3 and 4 contain samples containing DNA-DTE samples of the open (3) and closed isomer (4) of the switch in the original EtOH:TE buffer (1:1) mixture they were grown in as a comparison.

Fluorescence imaging was performed in a Nikon Eclipse LV100N POL microscope using filters of the following excitation and emission wavelength cut offs: λ_{exc} = 510-560 nm and λ_{em} = 580 nm. A selection of images is shown below.

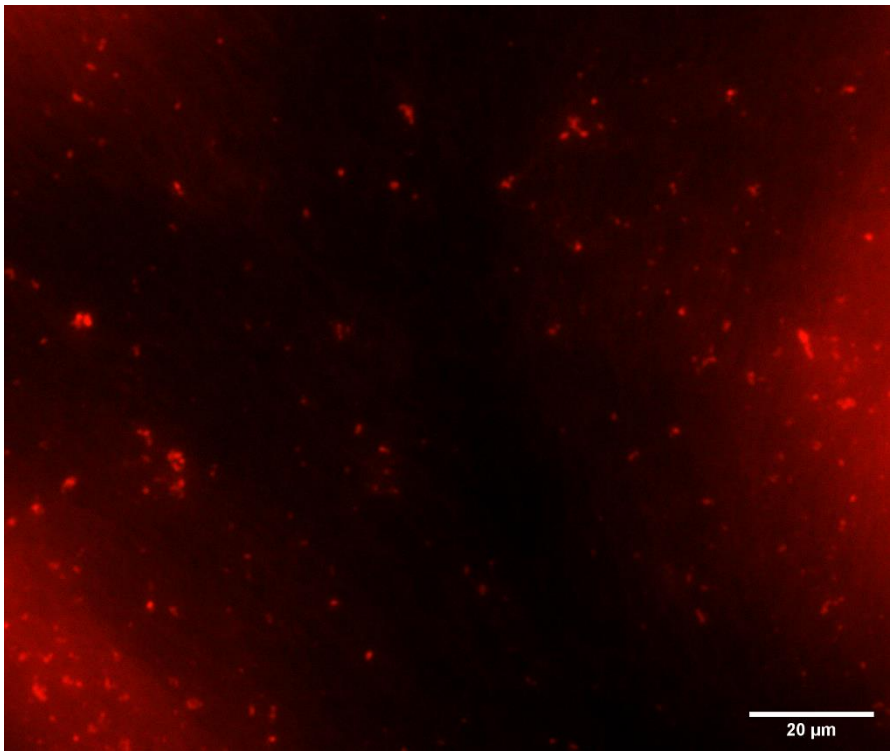

Figure S35. Fluorescence microscopy image of a sample taken from a two-month aged cylindrically shaped hydrogel stained with ethidium bromide.

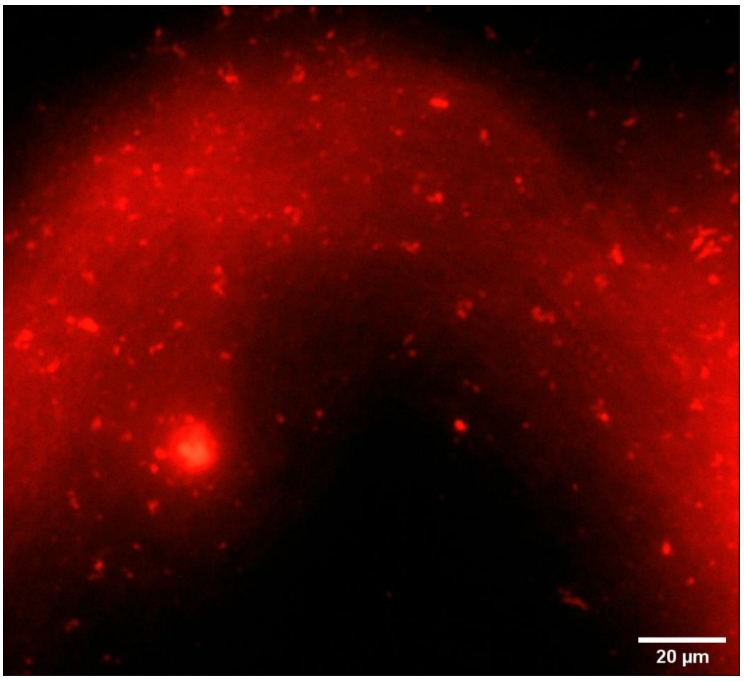

Figure S36. Fluorescence microscopy image of a sample taken from a two-month aged cylindrically shaped hydrogel stained with ethidium bromide.

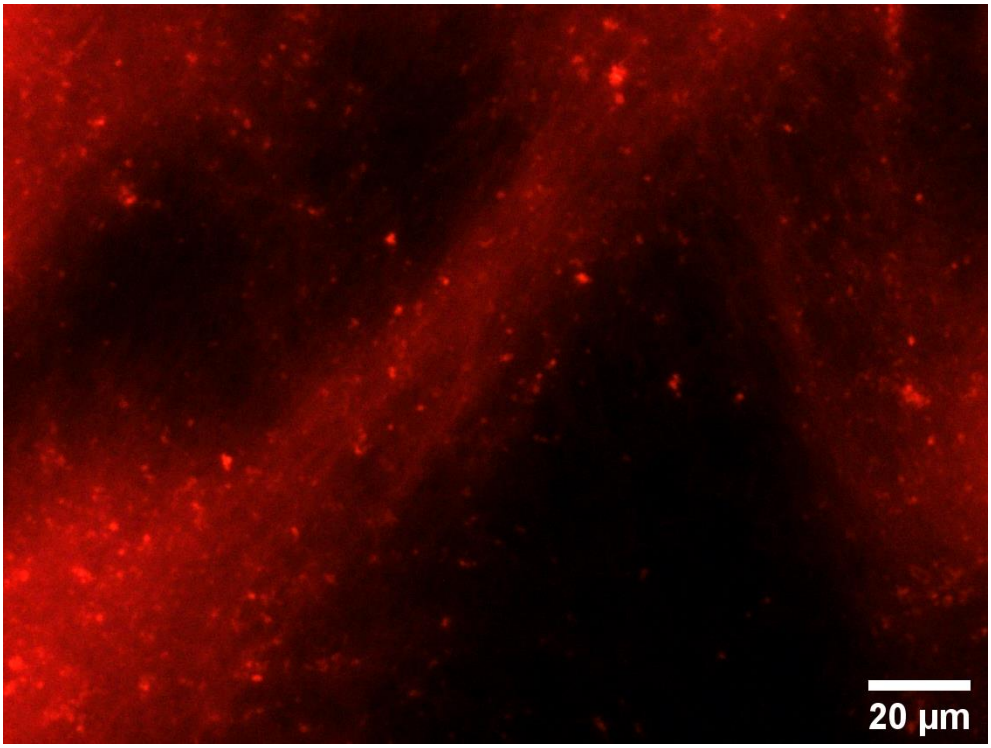

Figure S37. Fluorescence microscopy image of a sample taken from a two-month aged cylindrically shaped hydrogel stained with ethidium bromide.

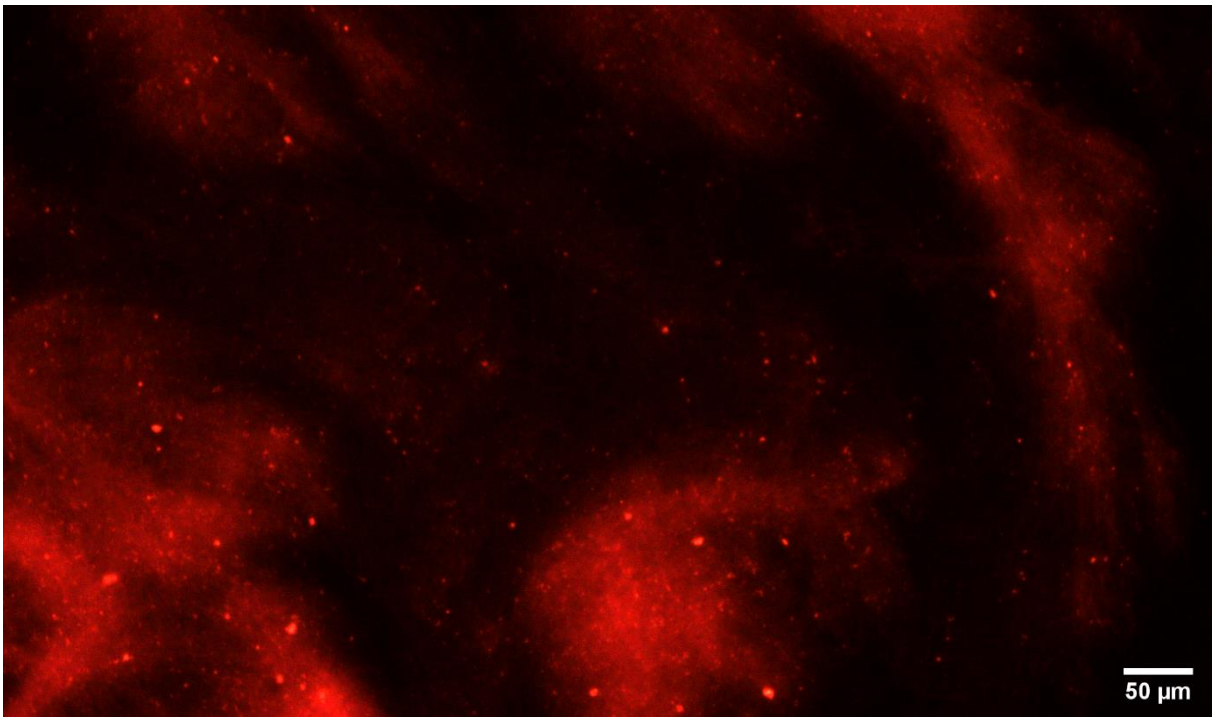

Figure S38. Fluorescence microscopy image of a sample taken from a two-month aged cylindrically shaped hydrogel stained with ethidium bromide.

8. Rheology

For rheology, a HR-3 Discovery Hybrid Rheometer with a 20 mm stainless steel flat plate with solvent trap (filled with EtOH) as top plate and a glass optical bottom plate were used. The measurements were performed at 25 °C.

An aged, cylindrically shaped gel was investigated and both the storage modulus (G') and the loss modulus (G") were recorded versus increasing oscillation strain (Figure S39 left). Repeated sweeps of the same sample show an increase in G', while the gel started to break earlier and G" stayed constant. Also, the photochemically torn strip shown in Figure 7 in the main text was measured accordingly (Figure S39 right). However, the sample was small and inhomogeneous due to the local photochemical manipulation and hence, the difference on G' between the irradiated and non-irradiated cannot be considered reliable. However, the irradiated gel shows an increase of G' over repeated sweeps and the same self-healing properties as the non-irradiated gel.

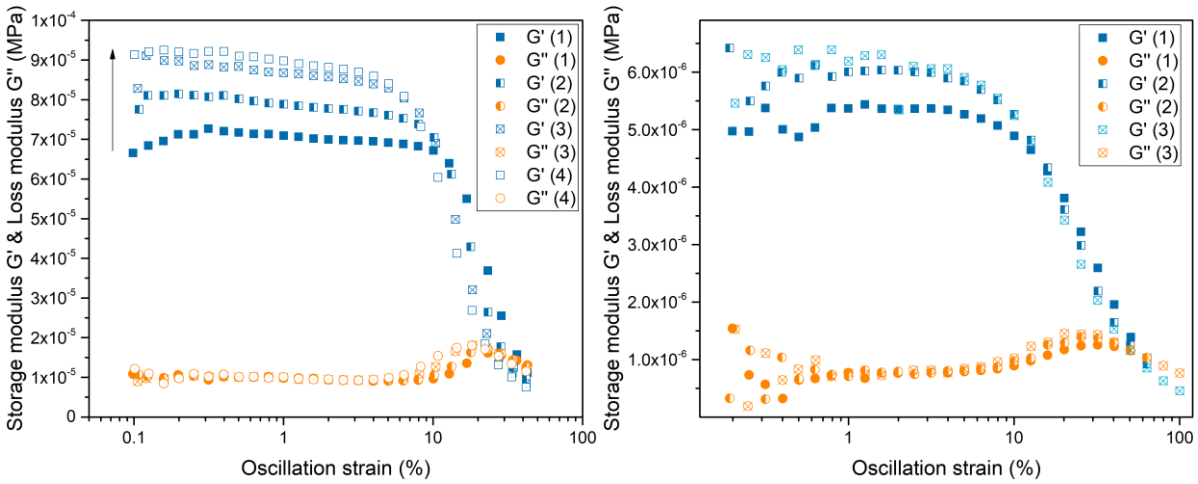

Figure S39. Storage modulus (G') and loss modulus (G") as a function of the applied oscillation strain. **Left**: Repeated sweeps (number in brackets) of the same gel before irradiation. **Right**: Repeated sweeps of the same gel after irradiation.

9. Additional experiments at the macroscopic scale

9.1.Casting hydrogels of different shapes

Samples containing **1o** and **dT$_{20}$** (1:1, EtOH:TE buffer 1:1, 600 µL) were prepared using the general procedure described in section S3 and after sonication transferred in vessels of different shape. An overview is displayed in Figure S40. The aging process was followed over time. While most of the shaped were formed after a few days, the cuboid needed a few weeks to be casted.

Figure S340 Samples containing **1o** and **dT$_{20}$** (1:1, EtOH:TE buffer 1:1, 600 µL) were refilled into different shapes directly after sonication.

9.1.1. Cylinder from **1o**

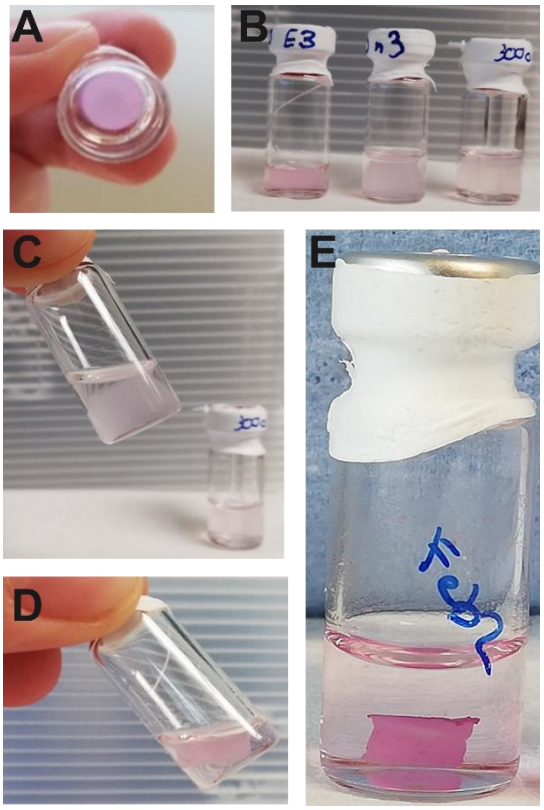

Figure S41. Samples containing **1o** and **dT$_{20}$** (1:1, EtOH:TE buffer 1:1, 600 µL) in a HPLC vial after 3 days (A, B), 6 days (C, D), and 4 weeks (E).

9.1.2. Cylinder from **1c**

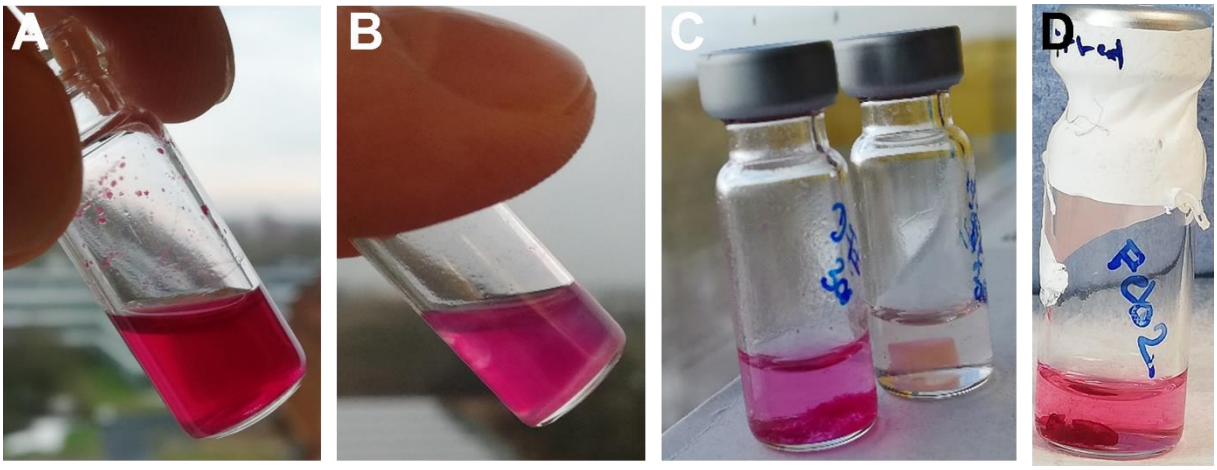

Figure S42. Samples containing **1c** and **dT$_{20}$** (1:1, PSS^{300}, EtOH:TE buffer 1:1, 600 µL) in a HPLC vial directly after sonication (**A**), after 1 week (**B**), 1 month (**C**), and 4 months (**D**).

9.1.3. Ring

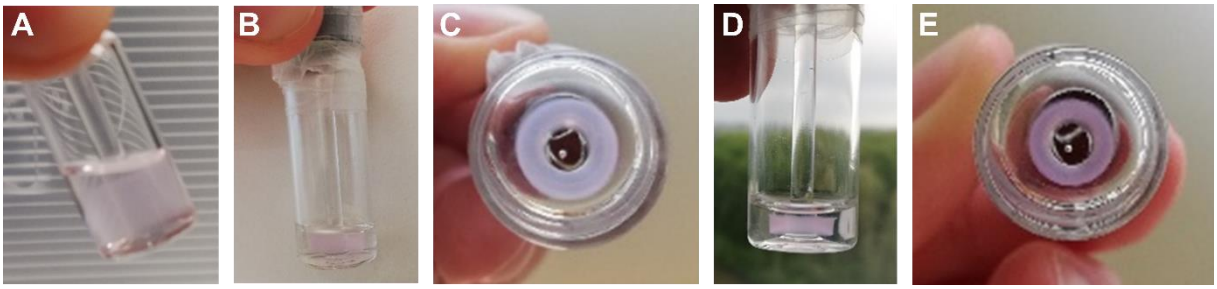

Figure S43. Samples containing **1c** and **dT$_{20}$** (1:1, EtOH:TE buffer 1:1, 600 µL) in a ring shaped vial after 3 days (**A**), 6 days (**B**, **C**), and 2 month (**D**, **E**).

9.1.4. Triangle

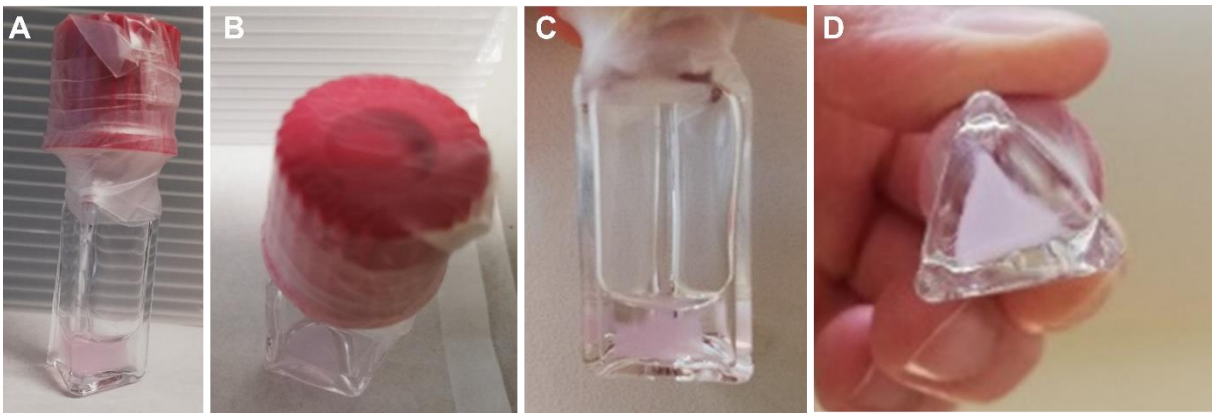

Figure S44. Samples containing **1c** and **dT$_{20}$** (1:1, EtOH:TE buffer 1:1, 600 µL) in a triangular vessel after 3 days (**A**, **B**), and 6 days (**C**, **D**).

9.1.5. Cube

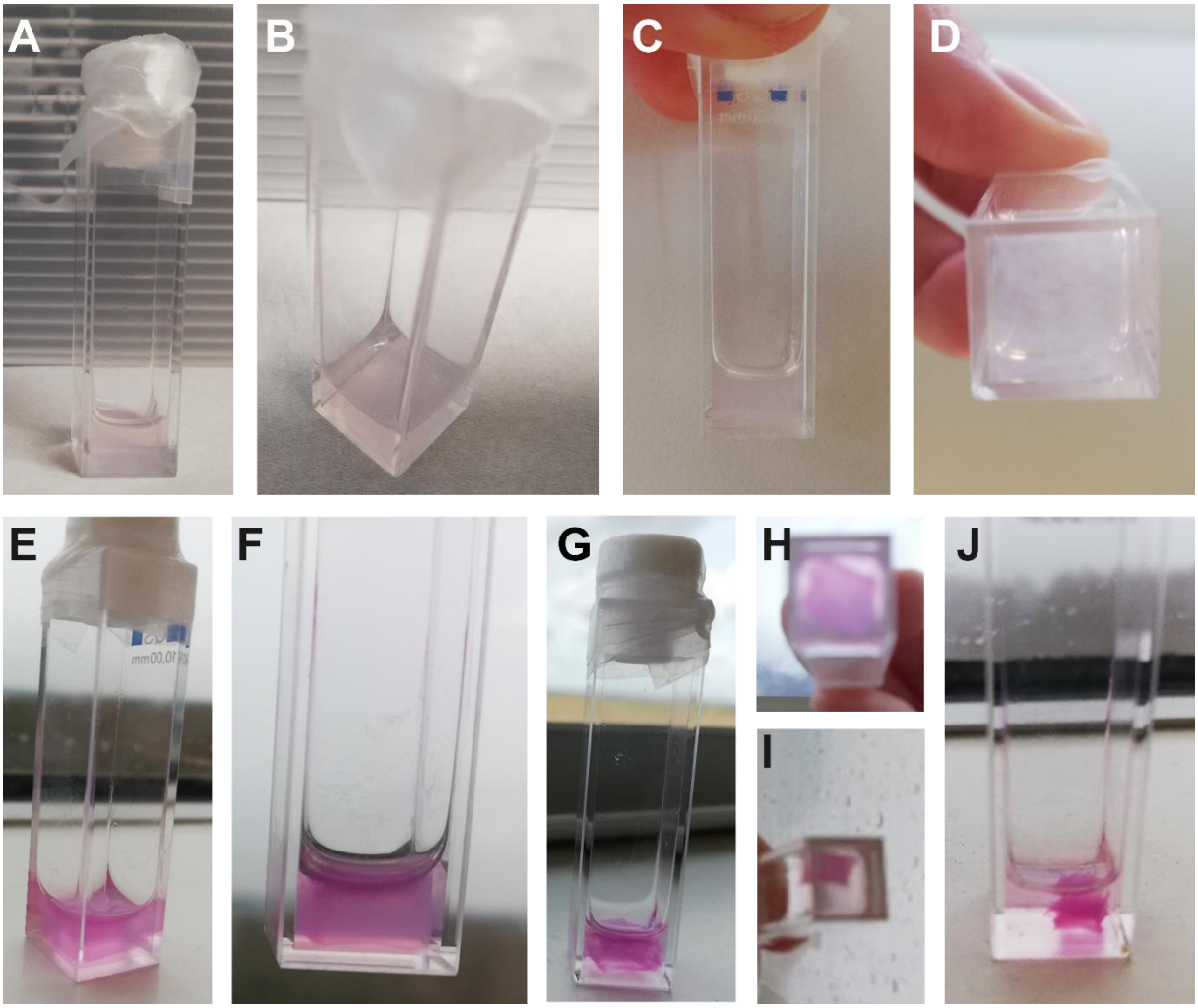

Figure S45. Samples containing **1o** and **dT$_{20}$** (1:1, EtOH:TE buffer 1:1, 600 µL) in a cuboid-shaped vessel after 3 days (**A**, **B**), and 6 days (**C**, **D**), 2 weeks (**E**, **F**), 3 weeks (**G**, **H**), and 6 weeks (**I**, **J**). Though, the sample was not irradiated, ambient light caused a colour-change over time penetrating through the quartz cuvette.

9.2.Exchanging the Solvent and the Vessel

Upon pipetting off the solvent, the EtOH:TE buffer 1:1 mixture the fibres were grown in, the structure collapses by *ca*. 50% appearing wet and jelly. Indeed, the residue can be pushed over a surface, stays intact, and responses elastic upon gently pressure (see Video1). Upon addition of pure TE buffer, the initial 3D structure was recovered (see Video1). However, the gel was now floating at the top of the solution indicating that it was still soaked in the original EtOH:TE buffer mixture of lower density (see Figure S46C, Video1). The sample was allowed to rest overnight in the dark during which time the 3D structure sank to the bottom of the vessel pointing towards a diffusion-controlled solvent exchange through the pores of the gel (see Figure S46C,D vial 2). In contrast, addition of heptane lead to irreversible collapse of the 3D architecture (see Figure S46C, D vial 1).

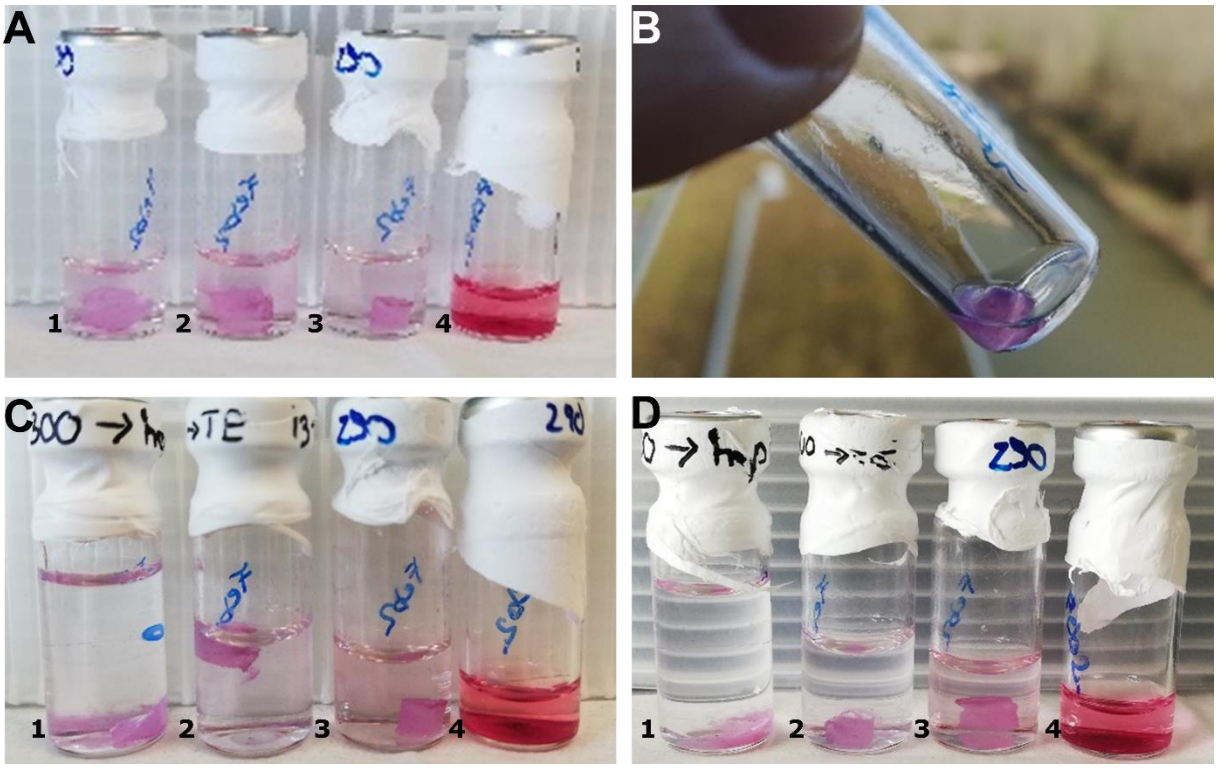

Figure S46. Exchanging the solvent in hydrogels grown from **1o** and **dT$_{20}$** (1:1, EtOH:TE buffer 1:1, 600 µL). **A**. Vial 1–3 contain hydrogels grown from **1o**, while vial 4 contains a samples of same age grown **1c** and **dT$_{20}$** (1:1, PSS^{300}, EtOH:TE buffer 1:1, 600 µL). **B**. Collapsed hydrogel from vial 2 without solvent. **C**. Vial 1–4 after addition of heptane to vial 1 and pure TE buffer to vial 2, while vial 3 and 4 stayed unaltered for comparison. **D**. Resting overnight lead to recovery of the hydrogel in vial 2, while heptane added to vial 1 destroyed the gel.

Moreover, transferring a cylindric hydrogel into a cuvette and storing it there did not influence the shape of the hydrogel (see Figure S4)

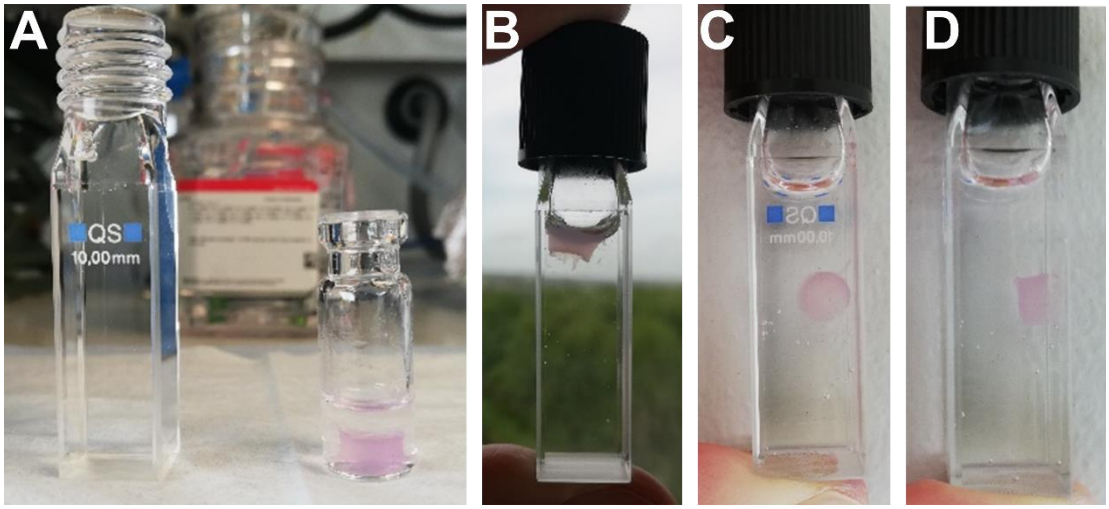

Figure S47. Transfer into a vessel of different shape combined with a solvent change to pure TE buffer did not influence the shape of the hydrogel. **A**. Initial containers. **B**. Directly after transfer. **C** and **D**. After 2 weeks stored in the dark. This sample was used for irradiation experiments (*cf*. section S8.4).

9.3.Drying the Hydrogel

To further elucidate the properties of the hydrogel, we fully removed the solvent. Drying of a cube-shaped gel on filter paper left a shape-resilient print on the paper while the buffer solution was soaked up (see Video 2).

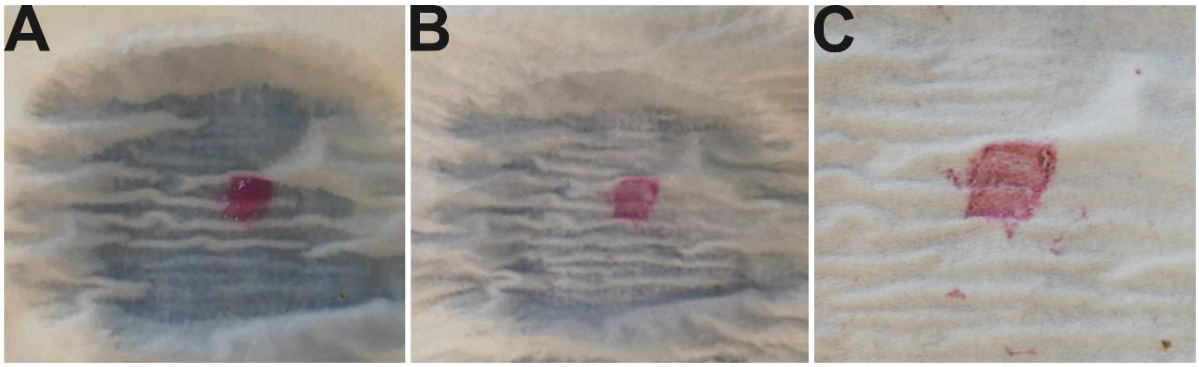

Figure S48. Drying of a cube-shaped hydrogel on filter paper over time (**A** to **C**).

9.4.Irradiation of the Hydrogel

Irradiation of the cylinder-shaped hydrogel, which was transferred and stored in a cuvette in the dark for two weeks (see Figure S49), with 300 nm light lead to shape-resilient shrinking and to a more brittle consistency. Analysis of the resulting 3D object by TEM showed that the twisted ribbons were still intact. Notably, the dense structure of the material lead to inhomogeneous, spatially limited photoswitching and the sample needed to be irradiated from several angles to ensure homogeneous shrinking (see Video 3). In contrast, irradiation with a 700 nm (M700F3, Thor Labs) and subsequently with a 526 nm LED (Sahlmann cooled 3 x LXML PM01 0100, 526 nm, FWHM = 35.1 nm, power output = 810 mW) for 2 h did not result in any change in shape or size.

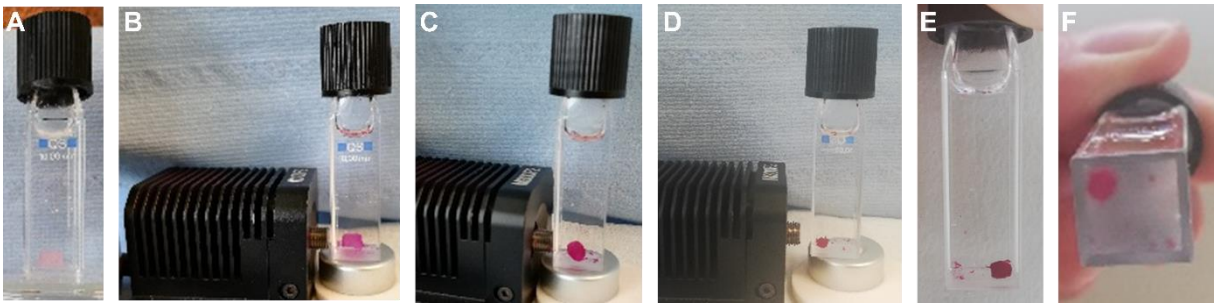

Figure S49. **A**. Initial hydrogel. **B**. After 4 min irradiation. **C**. After 1 h irradiation. **D**–**F**. After 4 h irradiation.

The same setup was used for the irradiation experiment displayed in Figure 5 in the main text (see Video 4).

9.5.Recovery of the Hydrogel

9.5.1. Melting

A hydrogel grown from **1o** and **dT$_{20}$** (1:1, EtOH:TE buffer 1:1, 600 µL) was step-wise heated in an oil bath to induce dissociation of the supramolecular assembly (Figure S50). At *ca*. 60 °C shrinking of the hydrogel was observed. At *ca*. 70 °C the 3D shape visibly collapsed, while at 80 °C melting and dissociation of the hydrogel could be observed. Further increasing of the temperature up to 100 °C did not dissolve the last aggregates. Hence, the sample was sonicated at 75 °C for 15 min and then cooled following the general procedure.

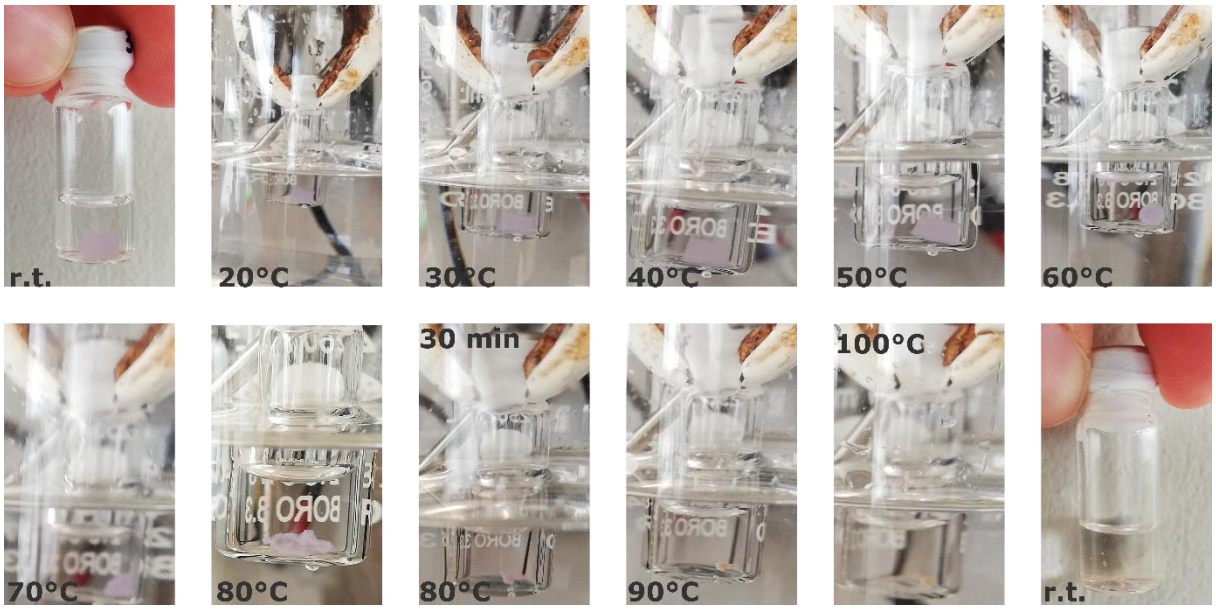

Figure S50. Stepwise heating of a cylinder-shaped hydrogel.

9.5.2. Irradiation with Green Light

Irradiation of samples grown from **1c** and **dT$_{20}$** (1:1, PSS^{300}, EtOH:TE buffer 1:1, 600 µL, *cf*. section S8.1.2.) with green light (45 min) lead to bleaching of the sample (see Figure S51).

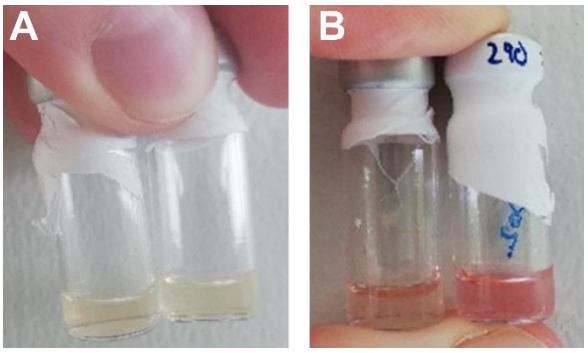

Figure S51. **A** and **B**. Different samples directly after irradiation with green light.

9.5.3. Recovered hydrogels

Both melted (*cf*. section S8.5.1., Figure S52 vial 1), lyophilized (not displayed), and irradiated (*cf*. section S8.5.3., Figure S52 vial 2–4) samples underwent the standard heating-cooling cycle (*cf*. section S3) and could be regrown.

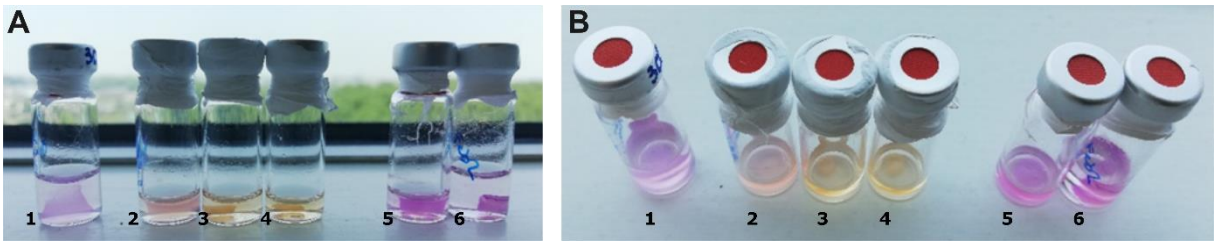

Figure S52. Recovered hydrogels after heat-induced melting (vial 1) and irradiation with green light (2-4) after 2 weeks as well as normally aged hydrogels after 4 weeks (vial 5) and 4 months (vial 6), respectively, as comparison (**A**. Side view, **B**. Top view).

10. References

1 L. N. Lucas, J. J. D. de Jong, J. H. van Esch, R. M. Kellogg and B. L. Feringa, Syntheses of Dithienylcyclopentene Optical Molecular Switches, *Eur. J. Org. Chem.*, 2003, **2003**, 155–166.